Dalton Transactions

ROYAL SOCIETY OF CHEMISTRY

PAPER

View Article Online
View Journal | View Issue

Open Access Article. Published on 09 June 2021. Downloaded on 9/19/2024 5:25:24 AM.
This article is licensed under a Creative Commons Attribution-NonCommercial 3.0 Unported Licence.

Check for updates

Cite this: *Dalton Trans.*, 2021, **50**, 9754

Non-palindromic (C^C^D) gold(III) pincer complexes are not accessible by intramolecular oxidative addition of biphenylenes – an experimental and quantum chemical study†

Wolfram Feuerstein and Frank Breher *

Received 23rd March 2021,
Accepted 9th June 2021

DOI: 10.1039/d1dt00953b

rsc.li/dalton

We herein report on the synthesis of biphenylenes substituted with a pyridine (N), a phosphine (P) and a carbene (C′) donor as well as a carbene donor with additional pyridine in the lateral position. We describe the synthesis and structures of derived gold(I) complexes, which we tried to use for the synthesis of non-palindromic [(C^C^D)Au^{III}] pincer complexes by means of an intramolecular oxidative addition of the strained biphenylene ring. However, the anticipated formation of gold(III) complexes failed due to kinetic and thermodynamic reasons, which we extensively investigated by quantum chemical calculations. Furthermore, we shed light on the oxidative addition of biphenylene to two different gold(I) systems reported in the literature. Our comprehensive quantum-chemical analysis is complemented by NMR experiments.

Introduction

Phosphorescent organic light-emitting diodes (OLEDs) based on transition metal complexes mainly incorporate the heavy metals iridium(III),[1–4] ruthenium(II)[5–7] or platinum(II).[8–13] However, in the last 15 years, structures based on gold(III) have gained increasing interest. Most of these systems incorporate the 2,6-diphenylpyridine based (C^N^C) pincer motif,[14–23] the rigid nature of which inhibits thermal relaxation.[24,25] In addition, the (C^N^C) pincer ensures a high ligand field splitting, which, upon photoexcitation, avoids the population of metal-centred d-states regularly seen to be responsible for non-radiative relaxation processes.[26,27]

Nevertheless, the (C^N^C) motif is by far not the only ligand suitable for the preparation of luminescent gold(III) structures. von Arx *et al.* described cyclometallated (C^C′) (C′ = N-heterocyclic carbene, NHC) gold(III) complexes with one or two phenyl alkynyl or pentafluorophenyl ligands.[28] There are also reports on biphenyldiyl (C^C) complexes of gold(III), the first by Usón *et al.* in 1980,[29] who prepared dibenzo stannoles and used the latter to transmetallate the biphenyl moiety to gold(III) salts. This approach was used by different groups for the preparation of luminescent gold(III) complexes.[30–32]

In 2015, Nevado and co-workers[33] described the non-palindromic[34] (C^C^N) analogue of the (C^N^C) pincer and proved that the corresponding gold(III) complexes outperform most palindromic congeners with regard to emission quantum yields.[35] In subsequent reports it was shown that the [(C^C^N)Au(III)] complexes differentiate from their palindromic counterparts with respect to chemical properties as well.[35–37] The (C^C^N) motif may be seen as a pincer variant of the bidentate biphenyl (C^C) ligand. Thus, only recently, we developed a synthetic access to pyridine and NHC substituted 2,2′-dihalobiphenyls, which are suitable pre-ligands for the preparation of highly luminescent (C^C^N) and (C^C^C′) gold(III) complexes by transmetallation of the respective stannoles.[38] In addition, we could show that 2,2′-dihalobiphenyls may be applied to palladium using a double oxidative addition – comproportionation sequence.[39]

However, in the course of searching for new variants for introducing (C^C^D)-based pincer ligands, we followed a different idea as well: In 2015, Dean Toste and co-workers showed a gold(I) NHC complex to be able to undergo an oxidative addition into the strained ring of biphenylene, thereby forming the corresponding cyclometalated [(C^C)Au^{III}] complex **3** (Chart 1A),[40] a reaction which was already shown to occur for group 10 metals.[41–45] Only shortly thereafter, the group of Didier Bourissou succeeded in a similar reaction employing a bidentate 1,2-diphosphano-1,2-dicarba-*closo*-dodecaborane ligand (Chart 1B).[46] Guy Bertrand and co-

Karlsruhe Institute of Technology (KIT), Institute of Inorganic Chemistry, Division Molecular Chemistry, Engesserstr. 15, 76131 Karlsruhe, Germany.
E-mail: breher@kit.edu

† Electronic supplementary information (ESI) available. CCDC 2018369–2018373. For ESI and crystallographic data in CIF or other electronic format see DOI: 10.1039/d1dt00953b

This journal is © The Royal Society of Chemistry 2021

Open Access Article. Published on 09 June 2021. Downloaded on 9/19/2024 5:25:24 AM.
This article is licensed under a Creative Commons Attribution-NonCommercial 3.0 Unported Licence.

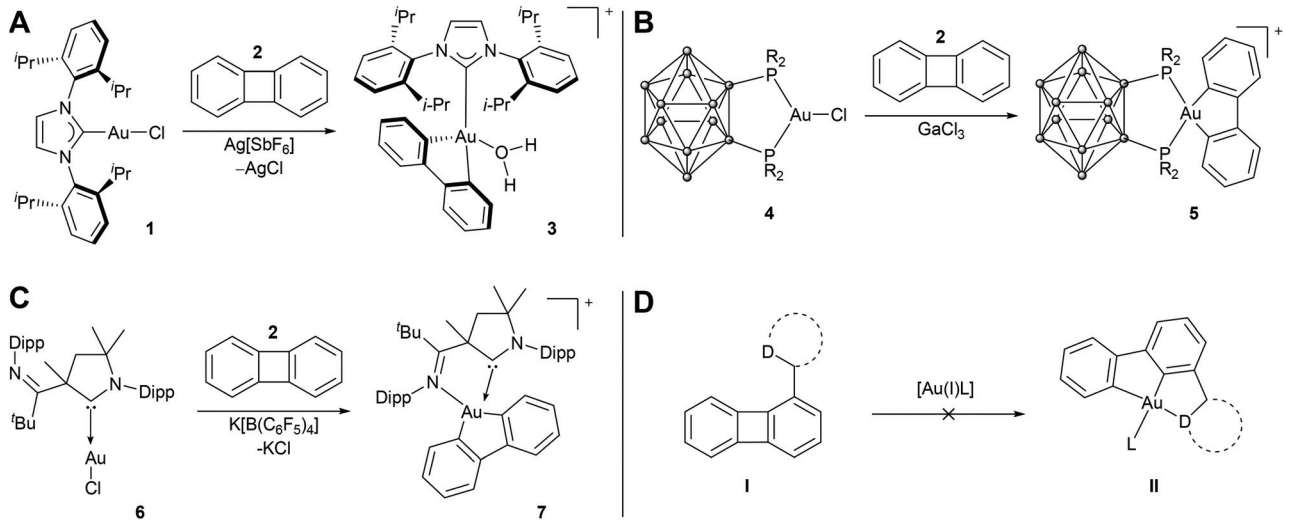

Chart 1 Oxidative addition of biphenylene (**2**) to gold(I) complexes reported in the literature (A–C) and the unsuccessful approach to prepare [(C^C^D)Au^{III}] complexes **II** by intramolecular oxidative addition of 2-substituted biphenylenes **I** investigated in this study (D). Anions are omitted for clarity. R = Ph, ^{i}Pr; ^{i}Pr = isopropyl; Dipp = 2,6-diisopropylphenyl; ^{t}Bu = *tert*-butyl; D = 2-pyridine, CH_2PPh_2, NHC; L = arbitrary neutral or anionic ligand or solvent molecule.

workers developed cyclic alkylamino carbenes (CAAC) substituted with an additional lateral donor, which enabled the oxidative addition of biphenylene to a gold(I) centre as well (Chart 1C).[47] A lateral amine-donor was also employed by Bourissou and co-workers for the oxidative addition of aryl iodide and biphenylene to a gold(I) phosphine complex.[48]

Thus, to broaden the opportunities to introduce biphenyl-based (C^C^D) pincers to gold(III), we focused on the synthesis of donor substituted biphenylenes, which should serve to prepare the anticipated complexes by means of an intramolecular oxidative addition of the biphenylene motif (Chart 1D). This approach was shown to succeed for [(C^C^N)Ir^{III}] complexes by Matsubara and co-workers.[49]

In this study, we describe the synthesis of such biphenylenes and discuss some of their gold(I) complexes. We show by comprehensive quantum chemical calculations that the intramolecular oxidative addition is impossible due to kinetic hindrance or the thermodynamic instability of reaction intermediates. Furthermore, we investigate the oxidative additions reported by Bertrand and Toste and discuss the conditions responsible for successful oxidative additions of biphenylenes to gold(I). NMR experiments complete our report.

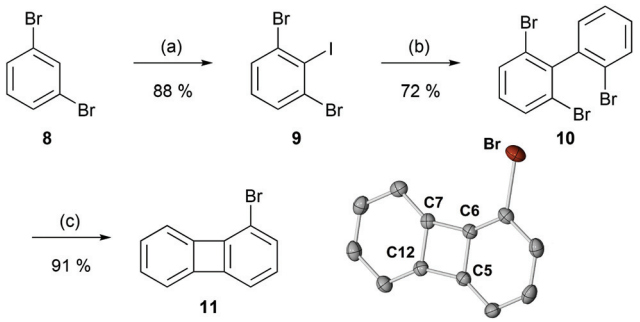

Scheme 1 Synthesis of 2-bromobiphenylene (**11**) starting from 1,3-dibromobenzene (**8**). Conditions: (a) (1) diisopropylamine, ^{n}BuLi, THF, −78 °C, 2 h (2) I_2, −78 °C → rt; (b) (1) ^{t}BuLi, THF, −100 °C, 1 h (2) 1,2-dibromobenzene, −78 °C → rt, 16 h; (c) (1) ^{n}BuLi, THF, −78 °C, 2 h (2) $ZnBr_2$, −50 °C (3) $CuCl_2$, −78 °C → rt, 16 h. Bottom right: Molecular structure of **11** in the solid state. Thermal ellipsoids are drawn at the 30% probability level. Hydrogen atoms are omitted for clarity. Only one molecule of the asymmetric unit is shown. Selected bond lengths (pm) and angles (°): C6–C7 149–6(3), C6–C5 142–0(3), C7–C12 142–0(3), C12–C5 151–4(4), C5–C6–C7 90–9(2), C6–C7–C12 89–9(2), and C7–C12–C5 90–1(2)–C12–C5–C6 89–1(2).

Results and discussion

Synthesis of biphenylene ligands

Starting from commercially available 1,3-dibromobenzene (**8**), we prepared 1-bromobiphenylene (**11**) according to a modified literature procedure (Scheme 1).[50–53]

Biphenylene **11** forms by the Cu^{II}-mediated ring closure of a zinkacyclopentadiene.[53] The latter is accessible *in situ* by the twofold lithiation of **10** and successive transmetallation with $ZnBr_2$. This kind of reaction is highly temperature-sensitive leading to a significantly reduced yield when upscaled (10 mmol ~ 50%).[50] However, we could overcome this problem by very slow addition of all reagents and by the use of a cooled (−75 °C) dropping funnel. Thus, we could perform this synthesis with excellent yields of 91% on scales >15 mmol.

1-Bromobiphenylene (**11**) served as the starting point to synthesize 2-(biphenylen-1-yl)pyridine (**12**) according to Koga *et al.*[49] and to obtain diphenylphosphine **15** in a three-step procedure (Scheme 2).

Open Access Article. Published on 09 June 2021. Downloaded on 9/19/2024 5:25:24 AM.
This article is licensed under a Creative Commons Attribution-NonCommercial 3.0 Unported Licence.

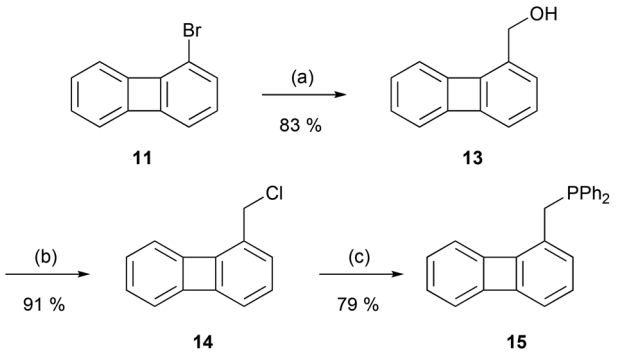

Scheme 2 Synthesis of phosphine **15**. Conditions: (a) (1) ^{t}BuLi, Et_2O, −78 °C, 1 h (2) paraformaldehyde, −78 °C → rt, 16 h; (b) thionylchloride, pyridine, Et_2O, reflux, 2 h; (c) (1) $HPPh_2$, ^{n}BuLi, THF, −78 °C → rt, 2 h (2) **14**, THF, −78 °C → rt, 16 h.

Furthermore, imidazole **16** was obtained in excellent yields by Pd-catalysed C–N-coupling using a Cu-based catalyst developed by Buchwald and co-workers (Scheme 3).[54]

Quaternization of **16** was accomplished using $[Et_3O][BF_4]$ or 2-bromomethylpyridine to obtain the imidazolium salts **17** and **18** (Scheme 4).

We anticipated pyridine substituted imidazolium salt **18** to serve as a tetradentate (C^C^C′^N) ligand able to stabilize cationic Au^{III} centres after oxidative addition into the biphenylene.[55]

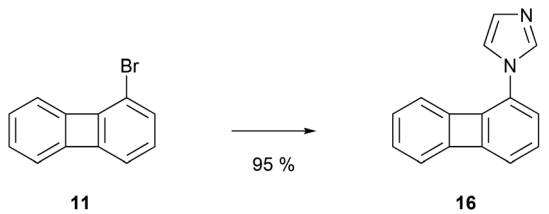

Scheme 3 Synthesis of imidazole **16**. Conditions: imidazole, Cu_2O (5 mol%), 4,7-dimethoxy-1,10-phenanthroline (15 mol%), Cs_2CO_3, PEG 400, butyronitrile, 110 °C, 24 h.

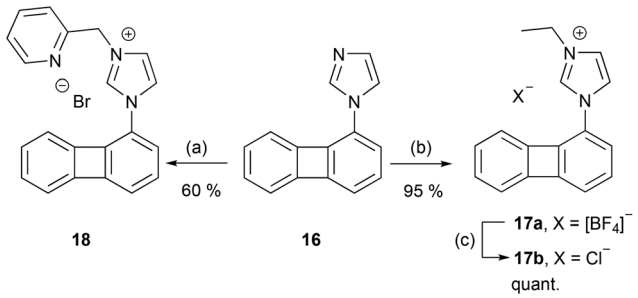

Scheme 4 Quaternization of imidazole **16**. Conditions: (a) (1) (2-bromomethyl)pyridine hydrobromide, $NaHCO_3$, H_2O, Et_2O, 0 °C, 10 min (2) **16**, MeOH, rt, 16 h; (b) $[Et_3O][BF_4]$, CH_2Cl_2, rt, 16 h; (c) Dowex® (chloride form), MeOH/H_2O (1 : 1), rt, 16 h.

Intramolecular oxidative addition

Gold(I) complexes. With the biphenylene based pre-ligands in hand, we synthesized Au^I complexes and tried to achieve the oxidative addition of the respective Au^I centre into the strained four-membered ring of the biphenylene unit.

Phosphine **15** readily displaces tetrahydrothiophene of [(tht)AuCl] to form complex **19** in excellent yields (Scheme 5). **19** crystallizes from CH_2Cl_2/*n*-hexane in the form of colourless prisms suitable for X-ray diffraction analysis (Fig. 1). The Au–P bond length is comparable to other Au(I) phosphine complexes.[56] The molecular structure does not indicate any interaction of the gold atom with the biphenylene unit. We also prepared NHC gold(I) complex **20** using imidazolium salt **17b** (Scheme 6). Crystals suitable for X-ray diffraction analysis were obtained from CH_2Cl_2/*n*-hexane (Fig. 2). In contrast to phosphine complex **19**, the gold atom of **20** is tilted in the same direction as the biphenylene unit and the C′–Au–Cl bond axis is slightly bent (177°). However, this is not indicative of a significant gold–biphenylene interaction.

Since neutral Au^I pyridine complexes are rare[57] due to the incompatibility of the hard pyridine donor and the soft gold(I) atom, we prepared cationic Au^I complex **21** with pyridine ligand **12** (Scheme 7).

[(C^C^N)Au^{III}]. Complex **21** did not undergo oxidative addition at room temperature. Heating (>60 °C) led to

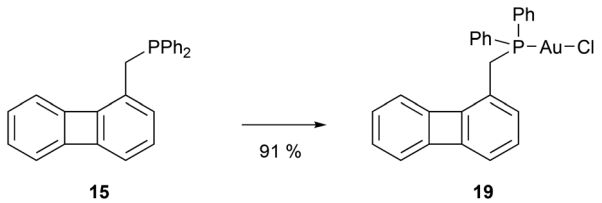

Scheme 5 Preparation of phosphine complex **19**. Conditions: [(THT)AuCl], CH_2Cl_2, rt, 24 h.

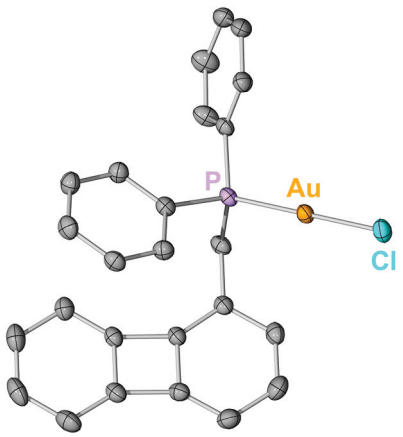

Fig. 1 Molecular structure of **19** in the solid state. Thermal ellipsoids are drawn at the 30% probability level. Hydrogen atoms are omitted for clarity. Selected bond lengths (pm) and angles (°): P–Au 222.5(1) and Au–Cl 227.8(1).

Open Access Article. Published on 09 June 2021. Downloaded on 9/19/2024 5:25:24 AM.
This article is licensed under a Creative Commons Attribution-NonCommercial 3.0 Unported Licence.

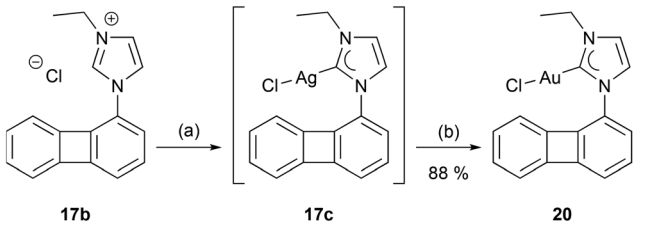

Scheme 6 Preparation of NHC gold(I) complex **20**. The silver NHC complex **17c** was prepared *in situ* and not isolated. Conditions: (a) Ag_2O, CH_2Cl_2, rt, 16 h; (b) [(THT)AuCl], 3 h.

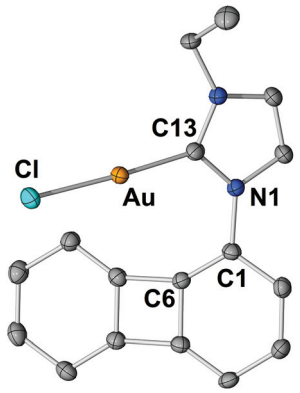

Fig. 2 Molecular structure of **20** in the solid state. Thermal ellipsoids are drawn at the 30% probability level. Hydrogen atoms are omitted for clarity. Selected bond lengths (pm) and angles (°): C13–Au 197.9(4), Au–Cl 228.6(1), and C6–C1–N1–C13 50.0(6).

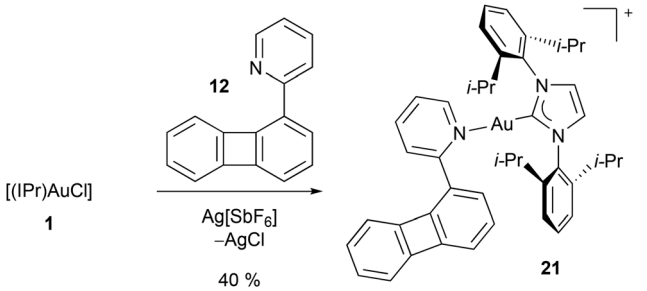

Scheme 7 Synthesis of cationic Au(I) complex **21**. Conditions: $Ag[SbF_6]$, CH_2Cl_2, rt, 24 h. The $[SbF_6]$-anion is omitted for clarity.

decomposition with the formation of elemental gold. Thus, we tried to synthesize Au^I complexes of pyridine ligand **12** *in situ* and to subsequently achieve an oxidative addition to form the desired $[(C^\wedge C^\wedge N)Au^{III}]$ complexes. We employed different Au^I sources; however, all approaches led to the formation of elemental gold, at least upon warming. Hence, [(CO)AuCl] loses CO when treated with **12** in CH_2Cl_2; however, after 3 h we could only isolate elemental gold. If reagents to abstract the chloride anion were added ($Ag[BF_4]$, $Ag[SbF_6]$, $K[B(C_6F_5)_4]$, and $Ag[Al(OC(CF_3)_3)_4]$[58]), the immediate formation of elemental gold was observed. The decomposition upon chloride abstraction was slightly slower in coordinating solvents (MeCN and DMF), but still quantitative after a couple of hours. The presence of oxygen or absence of light did not change any outcome. Furthermore, the addition of CsF, AgF or water did not avoid decomposition, let alone promote the desired oxidative addition. No reaction was observed when stirring gold phenylacetylide with **12** for seven days in CH_2Cl_2 or MeCN. Again, heating (oil bath or microwave) only led to the formation of elemental gold. Finally, we had no success with a bis acetonitrile Au^I complex described by Krossing and coworkers:[59] addition of **12** to $[(MeCN)_2Au][Al(OC(CF_3)_3)_4]$ in MeCN, CH_2Cl_2 or toluene produced elemental gold quantitatively.

$[(C^\wedge C^\wedge P)Au^{III}]$. Au(I) phosphine complex **19** did not undergo oxidative addition upon heating (decomposition >80 °C). **19** was subjected to different reaction conditions employing chloride abstraction reagents; however, we did not achieve the formation of the desired $[(C^\wedge C^\wedge P)Au^{III}]$ pincer complex (Scheme 8). Similar to the experiments using pyridine ligand **12**, in any case only the decomposition and formation of elemental gold after 2–6 h was observed. In THF, we observed polymerization upon chloride abstraction. In the presence of coordinating molecules like pyridine or benzalaniline, the cationic Au^I complexes formed as evidenced from NMR spectroscopy; however, upon heating only the formation of elemental gold was observed. The addition of $[^nBu_4N]Cl$ gave back reactant complex **19**.

$[(C^\wedge C^\wedge C')Au^{III}]$. Different chloride abstraction reagents (Tl[OTf], $Ag[SbF_6]$, and $K[B(C_6F_5)_4]$) were applied to NHC complex **20** in 1,2-difluorobenzene, MeCN, CH_2Cl_2 or DMSO. In all cases, a significant amount of elemental gold formed. However, in contrast to the previous experiments, in most cases the 1 : 2 NHC complex **23** could be isolated in low yields (Fig. 3). This may be indicative of a slightly longer lifetime of the intermediate cationic gold(I) species after chloride abstraction. As already reported for the previous experiments, the addition of CsF, AgF or water did not promote the desired oxidative addition, neither the presence of oxygen nor the

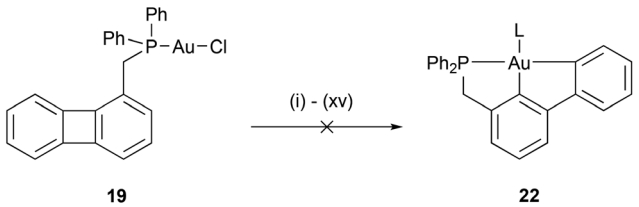

Scheme 8 Attempts to prepare [(C^C^P)Au(III)] complex **22**. L: Arbitrary ligand or solvent molecule. Conditions (all reactions at rt): (i) $Ag[BF_4]$, CH_2Cl_2; (ii) $Ag[BF_4]$, MeCN; (iii) $Ag[SbF_6]$, CH_2Cl_2; (iv) $K[B(C_6F_5)_4]$, CH_2Cl_2; (v) $Ag[Al(OC(CF_3)_3)_4]$, CH_2Cl_2; (vi) $Ag[SbF_6]$, MeCN; (vii) $K[B(C_6F_5)_4]$, MeCN; (viii) $Ag[Al(OC(CF_3)_3)_4]$, MeCN; (ix) $Ag[SbF_6]$, DMF; (x) Ag[SbF6] *or* $Ag[NTf2]$, CH_2Cl_2/MeCN (1 : 1); (xi) $Ag[SbF_6]$ *or* $AgNTF_2$, DMSO; (xii) Ag $[SbF_6]$ or $AgNTF_2$, MeCN/H_2O (1 : 1); (xiii) $Ag[SbF_6]$, pyridine, CH_2Cl_2; (xiv) benzalaniline, $Ag[SbF_6]$, CH_2Cl_2; (xv) $Ag[SbF_6]$, THF. The reactions failed in the presence of water as well.

Open Access Article. Published on 09 June 2021. Downloaded on 9/19/2024 5:25:24 AM.
This article is licensed under a Creative Commons Attribution-NonCommercial 3.0 Unported Licence.

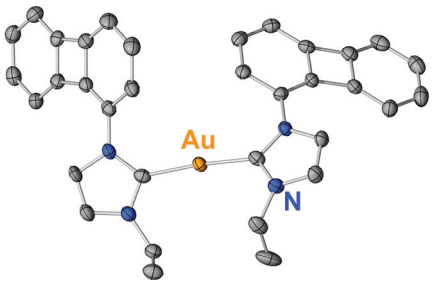

Fig. 3 Molecular structure of **23** in the solid state. Thermal ellipsoids are drawn at the 30% probability level. Hydrogen atoms and the triflate anion are omitted for clarity. Selected bond lengths (pm) and angles (°): C–Au 201.5(6), 201.6(7), and C–Au–C 173.6(3).

absence of light. Even at −90 °C, only decomposition was observed when treating **20** with a chloride abstraction reagent.

We tried to use imidazolium salt **18** with a lateral pyridine donor for the preparation of the corresponding Au^I and Au^{III} complexes as well. Unfortunately, even the isolation of the respective NHC Au^I complex failed due to decomposition over the course of two days after transmetallation of the Ag NHC complex of **18**. The addition of reagents for chloride abstraction after the *in situ* preparation of this NHC Au(I) complex resulted in the instantaneous decomposition to elemental gold as well.

Quantum chemical analysis

None of the presented attempts to prepare non-palindromic [(C^C^D)Au^{III}] complexes by intramolecular oxidative addition of biphenylene substituted ligands according to Chart 1D was successful. Thus, we were questioning ourselves whether kinetic or thermodynamic reasons were responsible for the failure of this approach and addressed this question by quantum chemical calculations.

By means of DFT calculations, Bourissou and co-workers investigated the oxidative addition of benzocyclobutenone to the gold atom of the cationic [(DPCb)Au^I]$^+$ complex, which forms by abstraction of chloride from [(DPCb)Au^ICl] (**4**, Chart 1B).[46] The flexibility of the bidentate DPCb diphosphine ligand is crucial for the success of this reaction: the bite angle may adjust according to the coordination tendencies of Au^I (linear) and Au^{III} (square-planar), thereby enabling the change of the coordination environment upon oxidative addition of biphenylene or benzocyclobutenone. Thus, they found a P–Au–P bite angle of 112° for [(DPCb)Au^I]$^+$ and 87° to 90° (isomer dependent) after oxidative addition and the formation of the respective Au^{III} complex. The ligands investigated in this study do not show this kind of flexibility; however, neither do the ligands used by Toste (Chart 1A)[40] or Bertrand (Chart 1C).[47]

We calculated the intramolecular oxidative addition of different biphenylene ligands according to Chart 1D at the RI[60]-TPSSh[61,62] D3(BJ)/def2-TZVPP[63–65] level of theory. The *meta*-GGA functional TPSS[62] was shown to yield reliable results for the structures of transition metal complexes in general[66,67] and in combination with dispersion correction (D3)[68] and Becke–Johnson damping (BJ)[69] for gold heteroatom bonds in particular.[70] Since we were interested in transition state barriers, we have chosen the hybrid variant TPSSh because activation barriers are often overestimated by pure functionals and the inclusion of exact exchange (10% for TPSSh) may give more reasonable results.[71] We considered solvent effects of CH_2Cl_2 by use of the SMD model (single point calculations using gas-phase optimized structures).[72]

We focused on pyridine, PPh_2 and NHC (methyl instead of ethyl in the calculated model) ligand as experimentally prepared and a hypothetical PMe_2 ligand. The Gibbs free energy of the transition state barrier ΔG_{TS} and the Gibbs free energy of the oxidative addition product ΔG_{II} for the different systems are listed in Table 1.

All calculated oxidative additions are thermodynamically favoured ($\Delta G_{II} < 0$), thus, the failure of the synthetic idea discussed in this study is not because of thermodynamic hindrance. The very low Gibbs free energy of the pyridine system (entry 1) is due to the instability of the hypothetical cationic Au^I complex of pyridine ligand **12**, which underlines a main problem of this synthetic approach: the biphenylene backbone coordinates *via* a donor – N, P or C′ – to the soft Au^I centre;

Table 1 Intramolecular oxidative addition of different biphenylene substituted ligands to Au(I) calculated at the RI-TPSSh-D3(BJ)/def2-TZVPP level of theory according to Chart 1D. Solvent effects of CH_2Cl_2 were taken into account by means of the SMD model (single point calculations only). Gibbs free energies of the transition state barrier ΔG_{TS} and the [(C^C^D)Au^{III}] product ΔG_{II} are given relative to the energy of the reactant complex **I** (G_A = 0). Electronic energies (kJ mol^{-1}) are given in parentheses

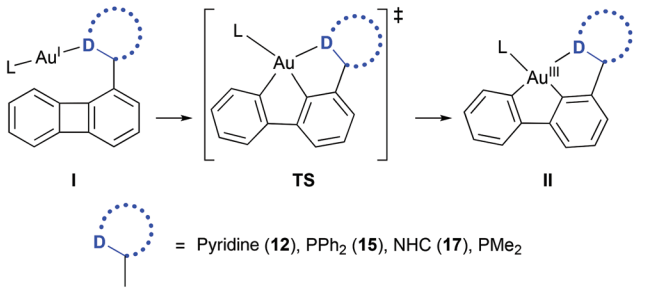

Entry	System	L	ΔG_{TS} (kJ mol^{-1})	ΔG_{II} (kJ mol^{-1})
1	Pyridine[a]	No	61 (60)	−160 (−153)
2	NHC[b]	MeCN	204 (191)	−53 (−49)
3	NHC	No	95 (86)	−101 (−98)
4	PPh_2	Cl^-	179 (199)	−56 (−66)
5	PPh_2	No	95 (92)	−61 (−59)
6	PMe_2	Cl^-	182 (192)	−60 (−71)
7	PMe_2	Pyridine	177 (176)	−63 (−49)
8	PMe_2	OTf^-[c]	171 (173)	−64 (−90)
9	PMe_2	MeCN	168 (169)	−60 (−48)
10	PMe_2	No	93 (89)	−68 (−57)

[a] No meaningful structure; the Au^I atom is rather coordinated in a η^2 manner by the biphenylene than by the pyridine's nitrogen atom. Thus, relative energies are of no meaning. [b] The calculation was done with a NHC complex with the methyl group instead of the ethyl group. [c] Coordination *via* oxygen atom.

 This journal is © The Royal Society of Chemistry 2021

Open Access Article. Published on 09 June 2021. Downloaded on 9/19/2024 5:25:24 AM.
This article is licensed under a Creative Commons Attribution-NonCommercial 3.0 Unported Licence.

however, this donor must be suitable to stabilize a hard Au^{III} centre after oxidative addition as well.

Neutral chloride complexes (entries 4 and 6) show barriers about twice as high compared to the hypothetical monocoordinated Au^{I} complexes without ligand or solvent molecule L (entries 5 and 10). However, even if the barriers are affected by the ligand L and decrease in the order Cl^{-} > pyridine > OTf^{-} > MeCN (entries 6–9), neither of the barriers is sufficiently low to kinetically allow the intramolecular oxidative addition. The biphenylene unit is not able to effectively bend the linear gold coordination towards a square-planar coordination. In the absence of any ligating molecule, the barrier is much lower (entries 3, 5 and 10), but the respective cationic Au^{I} complexes are purely hypothetical. Mono-coordinated gold(I) complexes instantaneously undergo reactions with surrounding molecules, mostly with reduction to elemental gold as it was found during all our experiments. Obviously, the biphenylene unit cannot effectively approach the Au^{I} centre to pre-empt decomposition pathways.

In summary, the intramolecular oxidative addition is thermodynamically favoured but fails due to the instability of mono coordinated Au^{I} complexes or the kinetic barrier accompanied by linearly coordinated Au^{I} centres.

The Bertrand-system

The oxidative addition of biphenylene to [(CAAC)Au^{I}] complexes described by Bertrand and co-workers (Chart 1C) is only possible in the case of CAAC ligands with an additional lateral donor.[47] After chloride abstraction, intermediary formed cationic Au^{I} complexes may be stabilized by coordination of π bonds as it is often seen in Au^{I} catalysis.[73] Thus, the linear coordination of biphenylene to Au^{I} is certainly the initial step of a C–C activation at the strained four-membered ring as it was already shown for other metals.[74,75] We optimized the structure of cationic [(CAAC)Au^{I}] biphenylene complex **6*** at the RI-TPSSh-D3(BJ)/def2-TZVPP level of theory and identified no interaction of the Au^{I} atom with the CAAC's lateral imine donor, thus the η^2 coordination of biphenylene is sufficient to form an adequately stabilized Au^{I} intermediate preventing decomposition to elemental gold (Scheme 9). The transition state of the oxidative addition $\mathbf{6_{TS}}$ is characterized by an imaginary stretching vibration of the four-membered biphenylene ring towards a five membered aura-cycle. We did not identify any interaction of the imine donor with gold at the transition state. Quite the contrary is true; the Au–N_{imine} distance is found to be longer at the transition state (d_{Au-N} = 343 pm) than in reactant complex **6*** (d_{Au-N} = 338 pm). Only for product **7**, the imine donor comes into play by stabilizing the Au^{III} centre (d_{Au-N} = 226 pm) and ensuring a square-planar coordination environment, thus, thermodynamically stabilizing the product of oxidative addition. Since Bertrand and co-workers report that no C–C bond activation occurs without a lateral donor at the CAAC ligand, the oxidative addition itself is maybe not thermodynamically favoured.

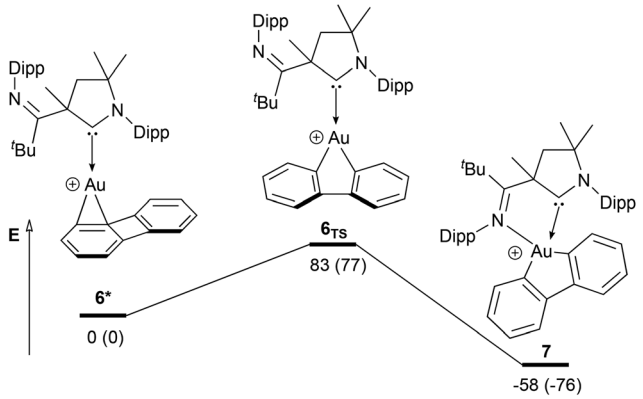

Scheme 9 Oxidative addition of biphenylene to [(CAAC)Au(I)] complex **6*** calculated at the RI-TPSSh-D3(BJ)/def2-TZVPP level of theory. Gibbs free energies (electronic energies in parentheses) are given in kJ mol^{-1} relative to reactant complex **6***. Solvent effects of CH_2Cl_2 were considered by means of the SMD model (single point calculations only).

The Toste system

At first sight, the former analysis contrasts with the oxidative addition of biphenylene to $[(IPr)Au^{I}]^{+}$ (Chart 1A). The IPr ligand employed by Toste and co-workers does not have any lateral donor like the CAACs employed in the Bertrand group, which is a requirement for the oxidative addition of biphenylene. However, Toste and co-workers report on water molecules coordinating to Au^{III} after C–C bond activation thereby stabilizing the Au^{III} oxidation state in a square-planar coordination environment. The authors used commercially available Ag[SbF_6] for chloride abstraction at [(IPr)AuCl] (**1**), which regularly contains significant amounts of water as we noticed during our own studies. Thus, we assumed the oxidative addition of biphenylene to $[(IPr)Au^{I}]^{+}$ may be only possible due to water impurities. To prove this assumption, we investigated this reaction by DFT calculations as well. However, since in the Toste case inter-molecular processes, *i.e.* water coordination or anion stabilizing effects may be of significant importance, for these calculations we have chosen to optimize all structures with the inclusion of solvent effects by the C-PCM model.[76] Furthermore, we did not only focus on the cationic Au(I)-species but included the $[SbF_6]^{-}$ anion as well. A comparison with calculations done with gas phase optimized structures is given in the ESI.†

After chloride abstraction, the cationic Au^{I} centre may be stabilized by the $[SbF_6]^{-}$ anion *via* coordination of one fluorine atom, by η^2 coordination of biphenylene or by a water molecule. Compared to the biphenylene coordination, the $[SbF_6]^{-}$ coordination is disfavoured by a Gibbs free energy of 33 kJ mol^{-1} (electronic energy: 98 kJ mol^{-1}). Water coordination is disfavoured as well by 26 kJ mol^{-1} (electronic energy: 36 kJ mol^{-1}), *i.e.*, water does not hinder oxidative addition. We emphasize at this point that we performed all our own oxidative addition experiments described in the foregoing section without success in the presence of water.

Open Access Article. Published on 09 June 2021. Downloaded on 9/19/2024 5:25:24 AM.
This article is licensed under a Creative Commons Attribution-NonCommercial 3.0 Unported Licence.

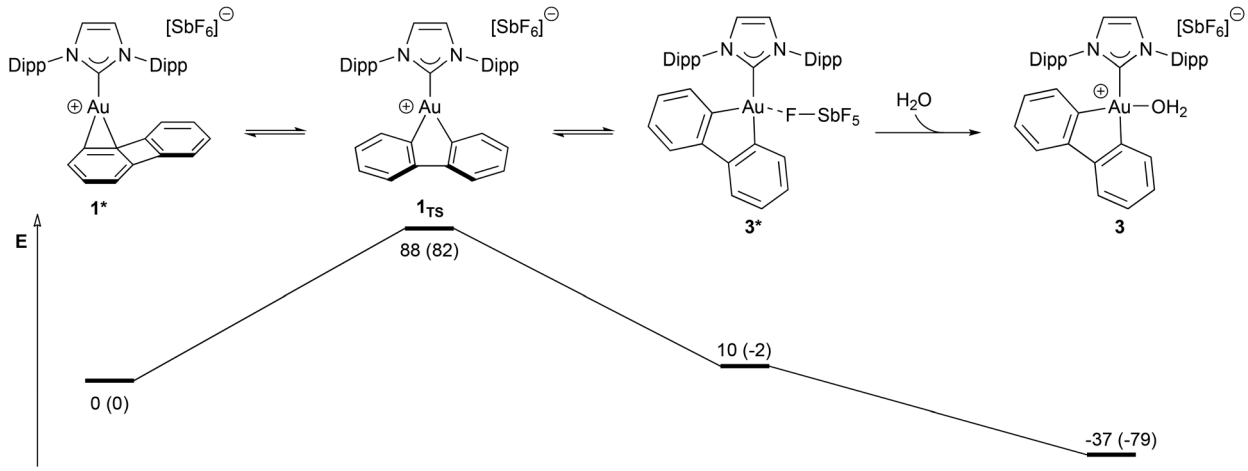

Scheme 10 Oxidative addition of biphenylene (**2**) to $[(IPr)Au(I)]^+$ (**1***) calculated at the RIJCOSX-TPSSh-D3(BJ)/def2-TZVPP level of theory. Gibbs free energies (electronic energies in parentheses) are given in kJ mol^{-1} relative to the reactant complex **1***. Solvent effects of CH_2Cl_2 were considered by means of the C-PCM model.

Starting from complex **1*** (Scheme 10), the barrier to the transition state $\mathbf{1_{TS}}$ of 88 kJ mol^{-1} (82 kJ mol^{-1}) is slightly higher compared to the Bertrand system shown in Scheme 9. Interestingly, the Gibbs free energy of the oxidative addition to form **3*** is found to be 10 kJ mol^{-1} (−2 kJ mol^{-1}); hence, the oxidative addition itself is not thermodynamically favoured. Confirming our assumption, the Gibbs free energy for displacing $[SbF_6]^-$ and coordination of one molecule water to the Au^{III} centre of **3*** is −37 kJ mol^{-1} making the whole process of oxidative addition thermodynamically favourable (electronic energy: −79 kJ mol^{-1}; see Computational Details for a discussion on the discrepancy between electronic and Gibbs free energy).

Thus, the calculations support our hypothesis that without water impurities the oxidative addition of biphenylene to $[(IPr)Au]^+$ (**1***) would probably not be possible.

Nevertheless, we were not satisfied by these pure quantum chemical findings. Therefore, we performed the oxidative addition of biphenylene to $[(IPr)Au^I]^+$ by ourselves in dry and wet CD_2Cl_2 according to the procedure of Toste and coworkers, using meticulously dried $Ag[SbF_6]$. We monitored the reaction *via* ^{1}H NMR spectroscopy (Fig. 4).

After chloride abstraction in dry CD_2Cl_2, no change of the biphenylene's ^{1}H signals (2-position: δ = 6.65 ppm, 1-position: δ = 6.75 ppm) is observed after 120 min nor after control measurements at 24 h and 48 h. However, after 48 h, the majority of $[(IPr)Au^I]^+$'s signals had disappeared due to decomposition and the formation of elemental gold.

In wet CD_2Cl_2, the biphenylene's signals are notably affected: the signal of the protons at the 1-position broadens during the reaction indicating some dynamic process. Interestingly, in the high field region, there is no difference of

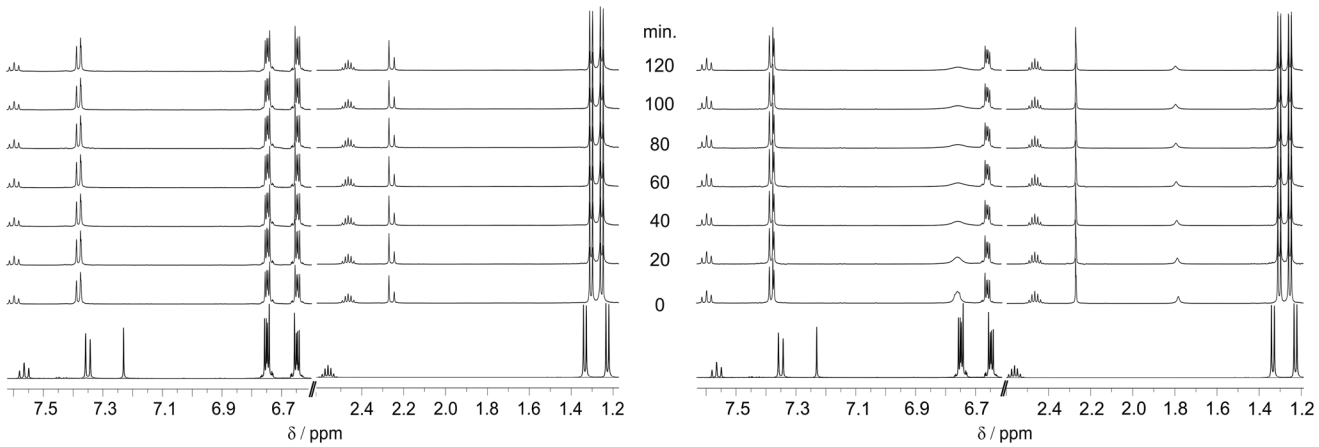

Fig. 4 ^{1}H NMR monitoring (500 MHz, CD_2Cl_2, 298.15 K) of the equimolar reaction of biphenylene (**2**) with $[(IPr)Au(I)]^+$ in the absence (left) and presence (right) of water (*ca.* 1.5 equivalents) (*cf.* Chart 1A and Scheme 10). The bottom spectra show the signals of biphenylene and [(IPr)AuCl] (**1**) before the addition of $Ag[SbF_6]$. After the addition of $Ag[SbF_6]$, the reaction mixture was instantaneously frozen and thawed just before the first NMR measurement (0 min).

Open Access Article. Published on 09 June 2021. Downloaded on 9/19/2024 5:25:24 AM.
This article is licensed under a Creative Commons Attribution-NonCommercial 3.0 Unported Licence.

the isopropyl group's signals (δ = 2.46, 1.30, 1.25 ppm) between dry and wet conditions. Thus, based on our NMR analysis, there are hints to dynamic processes enabled in the presence of water. However, we could not without doubt assign the NMR signature in wet CD_2Cl_2 to the oxidative addition of biphenylene and the clean formation of oxidative addition product **3*** and/or **3**. Therefore, a comprehensive clarification of the underlying mechanisms of this oxidative addition remains lacking.

Conclusions

The synthetic access to different substituted biphenylenes covering common donor motifs – phosphine, pyridine, and NHC – will probably be useful in the realm of transition metal complexes. However, our idea to use these compounds for the preparation of non-palindromic [(C^C^D)Au^{III}] complexes failed. The reasons for that are rooted in the kinetic hindrance of the intramolecular oxidative addition of biphenylene due to the linear coordination of Au^I that usually takes place. This avoids an effective bending of the biphenylene unit to the Au^I centre. By quantum chemical calculations, the oxidative addition is found to be only possible for monocoordinated Au^I complexes, which are purely hypothetical species. These results stand in line with other findings about the oxidative addition of Au^I to carbon–halogen bonds.[56]

The oxidative additions of biphenylene to Au^I complexes reported in the literature are enabled by additional factors and do not occur only due to the strain of the biphenylenes four-membered ring. In one case, a lateral imine donor (Bertrand) or the bite angle's flexibility of a diphosphine ligand (Bourissou) stabilizes the Au^{III} centre after oxidative addition. In the other case, water, which is a donor too hard to coordinate to the soft Au^I atom, enables dynamic processes and probably stabilizes a hard Au^{III} centre after the oxidative addition of biphenylene, as it is in accordance with our DFT calculations. However, our NMR experiments do not conclusively prove this assumption.

Thus, our study besides many others shows the versatility of the chemistry of gold; however, even if there are reports on catalytic transformations involving oxidative additions to Au^I, this kind of reaction still remains a phenomenon enabled by suitable conditions or specifically tailored ligands rather than being a common process.[77]

Experimental

General details

Manipulations were performed under a dry and oxygen-free argon or nitrogen atmosphere using standard Schlenk techniques.[78] Solvents were dried and degassed. All reagents were purchased from commercial sources and used as received except for $Ag[SbF_6]$ which was recrystallized from dry toluene and dried *in vacuo* at 120 °C for three hours. 1-Pyridylbiphenylene (**12**) was prepared according to a literature procedure.[49] Solution NMR spectra were recorded at 298.15 K using Bruker Avance Instruments operating at ^1H Larmor frequencies of 300, 400 or 500 MHz; chemical shifts are given in parts per million (ppm) relative to TMS for ^{13}C and ^1H, to H_3PO_4 for ^{31}P. NMR samples were prepared in oven-dried 5 mm NMR tubes. Air or moisture sensitive samples were prepared inside a glovebox using screw cap or Young valve NMR tubes or by vacuum transfer of the solvent to the samples and melting off the NMR tube.

IR spectra were recorded on a Bruker Alpha FT-IR spectrometer using the ATR technique (attenuated total reflection) on the bulk material, and the data are quoted in wavenumbers (cm^{-1}).

Mass spectra were recorded using a Varian MAT 3830 (70 eV) by electron ionization (EI).

Elemental analyses were done by the institutional technical laboratories of the Karlsruhe Institute of Technology (KIT).

Melting points were measured with a Thermo Fisher Scientific digital melting point apparatus of the IA9300 series and are not corrected.

Synthesis

1,3-Dibromo-2-iodobenzene (9). The synthesis was done according to a modified literature procedure.[51] At −78 °C 1.6 M ^{n}BuLi in hexane (10.24 g, 160.0 mmol, 100.0 ml, 1.00 eq.) was added dropwise under stirring to a solution of diisopropylamine (16.20 g, 160 mmol, 22.81 ml, 1.00 eq.) in THF (100 ml). 1,3-Dibromobenzene (**8**) (34.31 g, 145 mmol, 17.58 ml, 1.00 eq.) was added dropwise upon which a white precipitate formed. After stirring for 2 h at −78 °C, the mixture was treated with I_2 (38.64 g, 152 mmol, 1.05 eq.) in THF (50 ml). The cooling was removed, and the reaction was allowed to warm to room temperature. All solvents were removed *in vacuo* and the residue taken up in Et_2O (50 ml). The ethereal phase was washed with conc. $Na_2S_2O_{3(aq)}$ (3 × 60 ml) and water (3 × 60 ml), dried over $MgSO_4$ and evaporated to dryness. Recrystallization from boiling EtOH gave 46.2 g colourless plates (88%). Analytical data were in accordance with the literature.[51]

2,2′,6-Tribromobiphenyl (10). The synthesis was done according to a modified literature procedure.[51,52] At −100 °C 0.8 M ^{t}BuLi in pentane (19.17 g, 50.00 mmol, 62.5 ml, 2.00 eq.) was slowly (~20 ml h^{-1}) added under stirring to a solution of **9** (9.05 g, 25.00 mmol, 1.00 eq.) in THF (150 ml). Stirring was continued for 1 h and then 1,2-dibromobenzene (11.80 g, 50.00 mmol, 1.00 eq.) in THF (150 ml) was added dropwise. Stirring was continued and the mixture was allowed to warm to room temperature over the course of 16 h. Water (100 ml) was added and the aqueous phase was extracted with EtOAc (3 × 100 ml). The combined organic layers were washed with conc. $NaCl_{aq}$ and dried over $MgSO_4$. After evaporation of all volatiles *in vacuo* the residue was purified by column chromatography (SiO_2, cyclohexane) to obtain 7.04 g (72%) of a colourless solid. R_f = 0.38 (SiO_2, cyclohexane). Analytical data were in accordance with the literature.[51]

1-Bromobiphenylene (11). The synthesis was done according to a modified literature procedure.[50,53] At −78 °C 1.6 M ^{n}BuLi

Open Access Article. Published on 09 June 2021. Downloaded on 9/19/2024 5:25:24 AM.
This article is licensed under a Creative Commons Attribution-NonCommercial 3.0 Unported Licence.

in hexane (1.01 g, 15.75 mmol, 9.85 ml, 2.10 eq.) was added dropwise to a solution of **10** (7.5 mmol, 2.93 g, 1.00 eq.) in THF (100 ml). The solution was stirred for 2 h at −78 °C. Then a solution of $ZnBr_2$ (1.86 g, 8.25 mmol, 1.10 eq.) in THF (30 ml) was added and the resulting mixture stirred for 2 h at −50 °C. It was re-cooled to −78 °C and then transferred to a dropping funnel which was cooled to −75 °C by means of a cooling mantle. The solution was added over the course of three hours to a continuously stirred suspension of $CuCl_2$ (3.03 g, 22.5 mmol, 3.00 eq.) in THF (100 ml) at −78 °C. After complete addition, the mixture was stirred for additional 2 h at −78 °C and then allowed to warm to room temperature overnight. The mixture was hydrolyzed with 4 M HCl_{aq} (100 ml) and extracted with toluene (5 × 20 ml). The combined organic phases were washed with conc. $NaCl_{aq}$ and dried over $MgSO_4$. After evaporation of all volatiles the residue was filtered through a plug of Celite, the plug extracted with cyclohexane (250 ml), and the combined extracts evaporated to dryness to obtain 1.58 g of **11** (91%) as a yellow oil. The latter solidified after a couple of months giving crystals suitable for X-ray diffraction analysis. Analytical data were in accordance with the literature.[50,53]

Biphenylen-1-ylmethanol (13). In a Schlenk flask 1-bromobiphenylene (**11**) (960 mg, 4.15 mmol, 1.00 eq.) was dissolved in Et_2O (50 ml) and cooled to −78 °C. Under stirring 1.7 M ^{t}BuLi in pentane (585 mg, 9.13 mmol, 2.20 eq.) was added dropwise and the resulting orange solution was stirred for 1 h at −78 °C. Paraformaldehyde (249 mg, 8.30 mmol, 2.00 eq.) was added in small portions and stirring was continued for 1 h after which the mixture was allowed to warm to room temperature overnight. Water (50 ml) was added and the ethereal phase separated. The aqueous phase was extracted with EtOAc (3 × 20 ml) and the combined organic phases washed with conc. $NaCl_{aq}$, dried over $MgSO_4$ and evaporated to dryness. The residue was purified by column chromatography (SiO_2, cyclohexane/EtOAc = 3/1) to yield 574 mg of **13** (76%) as a white solid. $\boldsymbol{R_f}$ = 0.34 (SiO_2, cyclohexane/EtOAc = 3/1). **M.p.** = 76 °C. **^{1}H NMR** (300 MHz, CD_2Cl_2): δ = 6.78–6.71 (m, 3 H), 6.69–6.62 (m, 3 H), 6.56 (dt, J = 6.6, 0.7 Hz, 1 H), 4.52 (d, J = 5.3 Hz, 2 H, CH_2OH), 1.83 (t, J = 5.6 Hz, 1 H, CH_2O*H*). **^{13}C NMR** (75 MHz, CD_2Cl_2): δ = 151.8 (C_q), 151.6 (C_q), 151.6 (C_q), 148.5 (C_q), 132.3 (C_q), 129.3 (CH), 128.9 (CH), 128.7 (CH), 127.2 (CH), 118.8 (CH), 117.9 (CH), 116.8 (CH), 62.5 (CH_2OH). **IR (ATR):** $\tilde{\nu}$/cm^{-1} = 3272 (vw), 3180 (vw), 3059 (vw), 3027 (vw), 2891 (vw), 2839 (vw), 1908 (vw), 1881 (vw), 1835 (vw), 1786 (vw), 1590 (vw), 1499 (vw), 1456 (vw), 1444 (w), 1409 (w), 1386 (vw), 1346 (w), 1277 (w), 1203 (vw), 1149 (w), 1111 (vw), 1089 (vw), 1062 (w), 1044 (m), 1010 (w), 968 (w), 916 (vw), 885 (vw), 873 (vw), 795 (vw), 753 (m), 733 (vs), 699 (m), 652 (w), 622 (w), 578 (w), 530 (vw), 477 (w), 401 (vw), 383 (vw). **MS (EI, 70 eV)**, m/z (%): 182.1 (100%) $[M]^+$, 152.1 (70%) $[M - CH_3O]^+$. **Elemental analysis** calculated (%) for $C_{13}H_{10}O$: C 85.69, H 5.53, found: C 85.91, H 5.245.

1-(Chloromethyl)biphenylene (14). In a round bottom flask **13** (532 mg, 2.9 mmol, 1.00 eq.) was dissolved in Et_2O (20 ml). Under stirring thionylchloride (381 mg, 3.2 mmol, 0.23 ml, 1.10 eq.) was added dropwise. Then pyridine (15 mg, 0.2 mmol, 0.02 ml, 0.05 eq.) was added upon which a white precipitate formed. The mixture was stirred under reflux for one hour. Thionylchloride (381 mg, 3.2 mmol, 0.23 ml, 1.10 eq.) and pyridine (15 mg, 0.2 mmol, 0.02 ml, 0.05 eq.) were again added and the mixture stirred under reflux for one additional hour. Water (20 ml) was added and the mixture was extracted with Et_2O (3 × 10 ml). The combined organic phases were washed with conc. $NaCl_{aq}$, dried over $MgSO_4$ and evaporated to dryness. The crude product was purified by column chromatography (SiO_2, cyclohexane) to obtain 530 mg (91%) of a colourless solid. **M.p.** = 43 °C. **^{1}H NMR** (300 MHz, CD_2Cl_2): δ = 6.81–6.77 (m, 2 H), 6.77–6.75 (m, 1 H), 6.75–6.72 (m, 1 H), 6.74–6.65 (m, 1 H), 6.72–6.63 (m, 1 H), 6.59 (dd, J = 6.5, 1.0 Hz, 1 H), 4.41 (s, 2 H, CH_2Cl). **^{13}C NMR** (75 MHz, CD_2Cl_2): δ = 151.8 (C_q), 151.3 (C_q), 150.8 (C_q), 150.2 (C_q), 129.6 (CH), 129.2 (CH), 129.1 (CH), 128.7 (CH), 128.2 (CH), 119.1 (CH), 118.1 (CH), 117.5 (CH), 43.0 (CH_2Cl). **IR (ATR):** $\tilde{\nu}$/cm^{-1} = 3064 (vw), 3029 (vw), 2967 (vw), 2860 (vw), 1919 (vw), 1882 (vw), 1853 (vw), 1836 (vw), 1785 (vw), 1726 (vw), 1659 (vw), 1616 (vw), 1582 (vw), 1534 (vw), 1457 (vw), 1442 (w), 1410 (m), 1378 (w), 1343 (vw), 1323 (vw), 1274 (w), 1257 (m), 1246 (m), 1190 (vw), 1159 (vw), 1149 (m), 1111 (w), 1087 (w), 1055 (vw), 1018 (w), 969 (m), 916 (m), 893 (w), 865 (w), 805 (vw), 765 (m), 734 (vs), 713 (vs), 706 (vs), 679 (vs), 595 (s), 552 (m), 481 (vw), 399 (vw), 384 (w). **MS (EI, 70 eV)**, m/z (%): 200.0 (100%) $[M]^+$, 165.0 (100%) $[M - Cl]^+$. **Elemental analysis** calculated (%) for $C_{13}H_9Cl$: C 77.81, H 4.52, found: C 77.93, H 4.468.

(Biphenylen-1-ylmethyl)diphenylphosphane (15). At −78 °C diphenylphosphane (484 mg, 2.6 mmol, 0.45 ml, 1.00 eq.) in THF (50 ml) was treated dropwise with ^{n}BuLi in hexane (167 mg, 2.6 mmol, 1.63 ml, 1.00 eq.). The resulting red solution was stirred for 2 h at room temperature and then cooled to −78 °C. 1-(Chloromethyl)biphenylene (**14**) (530 mg, 2.6 mmol, 1.00 eq.) in THF (10 ml) was added dropwise and the mixture was stirred for 1 h at −78 °C, then warmed to room temperature and stirred overnight. Deoxygenated water was added and the resulting mixture was extracted with Et_2O (3 × 20 ml). The combined extracts were washed with deoxygenated water (20 ml) and the combined organic phases filtered through a plug of $MgSO_4$. Then all volatiles were removed *in vacuo* and the sticky residue was treated with *n*-pentane several times to obtain 720 mg (79%) of a yellowish solid. **M.p.** = 84 °C. **^{1}H NMR** (300 MHz, CD_2Cl_2): δ = 7.51–7.40 (m, 4 H), 7.37–7.29 (m, 6 H), 6.70–6.66 (m, 2 H), 6.65–6.56 (m, 2 H), 6.54–6.48 (m, 2 H), 6.46 (dt, J = 6.7, 1.0 Hz, 1 H), 3.26 (d, J = 0.6 Hz, 2 H, CH_2PPh$_2$). **^{13}C NMR** (75 MHz, CD_2Cl_2): δ = 151.7 (C_q), 151.5 (d, J_{C-P} = 1.8 Hz (C_q)), 151.1 (C_q), 150.2 (d, J_{C-P} = 6.0 Hz, C_q), 137.6 (d, J_{C-P} = 10.7 Hz, 2 C_q), 133.4 (d, J_{C-P} = 18.3 Hz, 4 CH), 130.7 (d, J_{C-P} = 6.6 Hz, CH), 129.6 (2 CH), 129.2 (d, J_{C-P} = 1.4 Hz, CH), 129.1 (d, J_{C-P} = 6.9 Hz, 4 CH), 128.6 (CH), 128.4 (CH), 128.0 (d, J_{C-P} = 8.7 Hz (C_q), 118.3 (d, J_{C-P} = 3.7 Hz, CH), 117.6 (CH), 115.9 (d, J_{C-P} = 2.1 Hz, CH), 32.5 (d, J_{C-P} = 12.9 Hz, CH_2PPh$_2$). **IR (ATR):** $\tilde{\nu}$/cm^{-1} = 3070 (vw), 3051 (vw), 2931 (vw), 2896 (vw), 2186 (vw), 2171 (vw), 2012 (vw), 1970 (vw), 1663 (vw), 1601 (vw), 1584 (vw), 1479 (vw), 1459 (vw), 1434 (w), 1414 (w), 1379 (vw), 1327 (vw), 1304 (vw), 1266 (vw), 1198

Open Access Article. Published on 09 June 2021. Downloaded on 9/19/2024 5:25:24 AM.
This article is licensed under a Creative Commons Attribution-NonCommercial 3.0 Unported Licence.

(vw), 1148 (vw), 1098 (vw), 1067 (vw), 1044 (vw), 1026 (vw), 999 (vw), 969 (w), 908 (vw), 889 (vw), 865 (vw), 836 (vw), 802 (vw), 766 (m), 735 (vs), 721 (m), 708 (w), 691 (vs), 612 (vw), 597 (vw), 580 (vw), 554 (vw), 506 (m), 497 (w), 472 (w), 429 (w), 396 (vw), 382 (vw). **MS (EI, 70 eV)**, *m/z* (%): 350.1 (42%) $[M]^+$, 165.1 (100%) $[M - PPh_2]^+$. **Elemental analysis** calculated (%) for $C_{25}H_{19}P$: C 85.69, H 5.47, found: C 85.70, H 5.480.

Biphenylenyl-1*H*-imidazole (16). A Schlenk tube was charged with imidazole (81.7 mg, 1.20 mmol, 1.20 eq.), Cu_2O (7.2 mg, 0.05 mmol, 0.05 eq.), 4,7-dimethoxy-1,10-phenanthroline (36 mg, 0.15 mmol, 0.15 eq.) and Cs_2CO_3 (456 mg, 1.40 mmol, 1.40 eq.). PEG-400 (0.1 ml), butyronitrile (1.0 ml) and 1-bromobiphenylene (**11**) (231 mg, 1.00 mmol, 1.00 eq.) were added and the resulting mixture was stirred at 110 °C for 24 h. After cooling to room temperature, the turbid orange–brown mixture was diluted with CH_2Cl_2 (10 ml), filtered through a plug of Celite® and the residue extracted with CH_2Cl_2 (50 ml). The yellow filtrate was evaporated to dryness and the resulting crude product was purified by column chromatography (SiO_2, CH_2Cl_2/MeOH = 10 : 1) to obtain 207 mg (95%) of a yellowish solid. R_f = 0.43. **M.p.** = 96 °C. **^{1}H NMR** (300 MHz, MeOH-*d*4): δ = 8.07 (dd, *J* = 1.4, 1.0 Hz, 1 H), 7.49 (t, *J* = 1.4 Hz, 1 H), 7.19 (dd, *J* = 1.5, 1.0 Hz, 1 H), 7.03–6.90 (m, 2 H), 6.87–6.83 (m, 2 H), 6.82–6.73 (m, 2 H), 6.66 (dd, *J* = 6.2, 1.2 Hz, 1H). **^{13}C NMR** (75 MHz, MeOH-*d*4): δ = 153.4 (C_q), 151.2 (C_q), 149.5 (C_q), 140.8 (C_q), 136.4 (CH), 132.1 (CH), 130.4 (CH), 130.3 (CH), 130.0 (CH), 128.1 (C_q), 121.6 (CH), 119.0 (2 CH), 118.9 (CH), 117.1 (CH). **IR (ATR)**: $\tilde{\nu}$/cm^{-1} = 3157 (vw), 3131 (vw), 3050 (vw), 2233 (vw), 2196 (vw), 2183 (vw), 2152 (vw), 2135 (vw), 2050 (vw), 2022 (vw), 2003 (vw), 1988 (vw), 1943 (vw), 1907 (vw), 1664 (w), 1603 (vw), 1588 (w), 1497 (s), 1445 (w), 1432 (w), 1386 (w), 1317 (m), 1297 (w), 1287 (w), 1261 (vw), 1244 (m), 1202 (vw), 1157 (w), 1099 (w), 1047 (m), 1021 (w), 973 (vw), 957 (w), 934 (vw), 903 (w), 879 (vw), 853 (vw), 816 (m), 795 (w), 753 (vs), 739 (vs), 726 (s), 698 (m), 653 (s), 623 (w), 614 (w), 590 (w), 522 (w), 484 (vw), 462 (vw), 426 (vw), 416 (vw), 403 (vw), 394 (vw). **MS (ESI)**, *m/z* (%): 219.1 (100%) $[M + H]^+$. **Elemental analysis** calculated (%) for $C_{15}H_{10}N_2$: C 82.55, H 4.62, N 12.84 found: C 82.10, H 4.448, N 12.67.

1-(Biphenylen-1-yl)-3-ethyl-1*H*-imidazol-3-ium tetrafluoroborate/chloride (17). In a Schlenk tube **16** (100 mg, 0.46 mmol, 1.00 eq.) and $[Et_3O][BF_4]$ (105 mg, 0.55 mmol, 1.20 eq.) were dissolved in CH_2Cl_2 (2 ml) and the resulting mixture was stirred overnight at room temperature. *n*-Hexane (20 ml) was added and the precipitating yellow solid was filtered, washed with water (5 ml) and dried *in vacuo*; 146 mg (95%) (**17a**).

To exchange $[BF_4]$ for chloride, **17a** (200 mg) was dissolved in MeOH (20 ml) and H_2O (8 ml) and passed through a column (2 cm inner diameter) packed with about 3 g of Dowex® (chloride form). The column was extracted with MeOH/H_2O (1 : 1) (3 × 20 ml) and the combined filtrates evaporated to dryness. The residue was taken up in CH_2Cl_2 (50 ml), dried over $MgSO_4$ and finally all solvent was removed under reduced pressure. After drying *in vacuo* 169 mg (quant.) of a yellowish solid were isolated (**17b**). **17a**: **M.p.** = 136 °C. **^{1}H NMR** (300 MHz, Aceton-*d*6): δ = 9.54 (t, *J* = 1.6 Hz, 1 H), 8.08 (s, 1 H), 8.08 (s, 1 H), 7.18 (dd, *J* = 8.8, 0.7 Hz, 1 H), 7.09 (dd, *J* = 8.8, 6.7 Hz, 1 H), 7.02–6.83 (m, 5 H), 4.57 (q, *J* = 7.3 Hz, 2 H, C*H*$_2$Me), 1.67 (t, *J* = 7.3 Hz, 3 H, CH$_2$C*H*$_3$). **^{13}C NMR** (75 MHz, Acetone-*d*6): δ = 153.1 (C_q), 150.8 (C_q), 147.9 (C_q), 142.8 (C_q), 135.4 (C_q), 132.4 (CH), 131.0 (CH), 130.2 (CH), 125.8 (C_q), 124.5 (CH), 122.2 (CH), 122.0 (CH), 120.1 (CH), 119.6 (CH), 119.1 (CH), 46.5 (CH_2), 15.5 (CH_3). **IR (ATR)**: $\tilde{\nu}$/cm^{-1} = 3156 (vw), 2575 (vw), 2516 (vw), 2501 (vw), 2451 (vw), 2386 (vw), 2325 (vw), 2282 (vw), 2265 (vw), 2232 (vw), 2221 (vw), 2207 (vw), 2184 (vw), 2176 (vw), 2148 (vw), 2115 (w), 2081 (vw), 2064 (w), 2019 (vw), 1990 (vw), 1965 (vw), 1956 (vw), 1941 (vw), 1926 (vw), 1902 (vw), 1889 (vw), 1861 (vw), 1665 (vw), 1603 (vw), 1576 (vw), 1548 (vw), 1464 (vw), 1445 (vw), 1418 (vw), 1320 (vw), 1277 (vw), 1192 (vw), 1159 (vw), 1047 (vs), 1033 (vs), 967 (w), 881 (vw), 863 (vw), 837 (w), 793 (vw), 746 (vs), 707 (vw), 696 (w), 670 (vw), 633 (w), 616 (w), 596 (vw), 585 (vw), 565 (w), 543 (w), 520 (m), 501 (w), 492 (w), 477 (w), 463 (vw), 452 (w), 443 (w), 432 (w), 422 (w), 409 (w), 400 (w), 385 (m). **MS (ESI)**, *m/z* (%): 247.1 (100%) $[M]^+$. **Elemental analysis** calculated (%) for $C_{17}H_{15}N_2BF_4$: C 61.11, H 4.53, N 8.38 found: C 60.09, H 4.329, N 8.37. **17b**: **M.p.** = 177 °C. **^{1}H NMR** (300 MHz, CD_2Cl_2): δ = 9.19 (t, *J* = 1.7 Hz, 1 H), 7.55 (d, *J* = 1.6 Hz, 2H), 7.03 (s, 1 H), 7.02 (d, *J* = 2.9 Hz, 1 H), 6.99–6.82 (m, 2 H), 6.82–6.76 (m, 3 H), 4.45 (q, *J* = 7.2 Hz, 2 H, C*H*$_2$Me), 1.63 (t, *J* = 7.3 Hz, 3 H, CH$_2$C*H*$_3$). **MS (ESI)**, *m/z* (%): 247.1 (100%) $[M]^+$. **Elemental analysis** calculated (%) for $C_{17}H_{15}N_2Cl$: C 72.21, H 5.35, N 9.91 found: C 72.19, H 5.151, N 9.73.

1-(Biphenylen-1-yl)-3-(pyridin-2-ylmethyl)-1*H*-imidazol-3-ium bromide (18). 2-(Bromomethyl)pyridine hydrobromide (122 mg, 0.48 mmol, 1.05 eq.) was treated with conc. $NaHCO_{3(aq)}$ (10 ml) and Et_2O (10 ml) at 0 °C and stirred for 10 min. The pink ethereal phase was separated, the aqueous phase was extracted with cold Et_2O (2 × 10 ml) and the combined organic phases were filtered. Under stirring a solution of **16** (100 mg, 0.46 mmol, 1.00 eq.) in MeOH (10 ml) was added. The volume of the resulting pink mixture was reduced to about 10 ml at 0 °C and the resulting solution was stirred overnight at room temperature. All volatiles were removed *in vacuo*, and the residue was taken up in CH_2Cl_2 (10 ml) and filtered. The filtrate was added dropwise to vigorously stirred Et_2O (50 ml) upon which a pink solid formed. The latter was separated by the use of a centrifuge, redissolved in CH_2Cl_2 and again added to vigorously stirred Et_2O. The solid was again separated by use of a centrifuge and dried *in vacuo*. 107 mg (60%) of a red, crystalline, very hygroscopic solid were obtained. **M.p.** = 115 °C. **^{1}H NMR** (300 MHz, CD_2Cl_2): δ = 11.19 (t, *J* = 1.6 Hz, 1 H), 8.58 (ddd, *J* = 4.8, 1.8, 0.9 Hz, 1 H), 8.03 (dd, *J* = 2.1, 1.5 Hz, 1 H), 7.98 (dt, *J* = 7.8, 1.1 Hz, 1 H), 7.81 (td, *J* = 7.7, 1.8 Hz, 1 H), 7.52 (t, *J* = 1.9 Hz, 1 H), 7.34 (ddd, *J* = 7.6, 4.9, 1.2 Hz, 1 H), 7.23 (dd, *J* = 8.8, 0.5 Hz, 1 H), 6.98 (dd, *J* = 8.8, 6.9 Hz, 1 H), 6.93–6.84 (m, 3 H), 6.79–6.74 (m, 1 H), 6.72 (dd, *J* = 6.9, 0.5 Hz, 1 H), 6.06 (s, 2 H, C*H*$_2$). **^{13}C NMR** (75 MHz, CD_2Cl_2): δ = 153.0 (C_q), 152.7 (C_q), 150.4 (C_q), 150.0 (CH), 147.2 (C_q), 141.8 (C_q), 138.5 (CH), 136.2 (CH), 132.3 (CH), 130.7 (CH), 129.8 (CH), 125.0 (CH), 124.9 (C_q), 124.7 (CH), 124.7 (CH), 121.2 (CH), 119.9 (CH), 119.4 (CH), 119.3 (CH), 118.7 (CH), 54.3 (CH_2). **IR (ATR)**: $\tilde{\nu}$/cm^{-1} = 3035 (vw), 2287 (vw), 2186

Open Access Article. Published on 09 June 2021. Downloaded on 9/19/2024 5:25:24 AM.
This article is licensed under a Creative Commons Attribution-NonCommercial 3.0 Unported Licence.

(vw), 2166 (vw), 2129 (vw), 2098 (vw), 2024 (vw), 1998 (vw), 1984 (vw), 1935 (vw), 1610 (vw), 1590 (vw), 1568 (vw), 1545 (w), 1468 (vw), 1437 (w), 1419 (w), 1367 (vw), 1331 (vw), 1267 (vw), 1229 (vw), 1189 (w), 1155 (vw), 1100 (vw), 1069 (vw), 1052 (vw), 1020 (vw), 996 (vw), 972 (vw), 875 (vw), 817 (vw), 796 (w), 741 (vs), 697 (m), 653 (m), 638 (m), 619 (m), 595 (w), 582 (w), 520 (w), 476 (w), 464 (w), 449 (w), 431 (w), 422 (w), 402 (w), 393 (w), 385 (w). **MS (ESI)**, *m/z* (%): 310.1 (100%) $[M]^+$. **Elemental analysis** calculated (%) for $C_{21}H_{16}N_3Br$: C 64.63, H 4.13, N 10.77 found: C 64.88, H 4.041, N 10.99.

(Biphenylen-1-ylmethyl)diphenylphosphane gold(I)chloride (19). [(THT)AuCl] (80 mg, 0.25 mmol, 1.00 eq.) and **15** (88 mg, 0.25 mmol, 1.00 eq.) were dissolved in CH_2Cl_2 (5 ml). After stirring for 24 h the mixture was filtered and evaporated to dryness. The residue was washed with *n*-hexane (2 × 10 ml), dried *in vacuo*, and re-dissolved in CH_2Cl_2 (2 ml). The solution was layered with *n*-hexane upon which colourless prisms formed after one week. The supernatant solution was removed and the crystals were washed with *n*-hexane (10 ml) and dried *in vacuo*; 132 mg (91%). **M.p.** = 139 °C. **^{1}H NMR** (300 MHz, CD_2Cl_2): δ = 7.75–7.62 (m, 4 H), 7.57–7.40 (m, 6 H), 6.74–6.67 (m, 1 H), 6.69–6.57 (m, 3 H), 6.58 (dt, J = 4.6, 1.5 Hz, 1 H), 6.54 (ddd, J = 6.6, 1.8, 0.9 Hz, 1 H), 6.29 (dtd, J = 6.6, 1.0, 0.5 Hz, 1 H), 3.61 (d, J = 12.0 Hz, 2 H, CH_2PPh_2). **^{13}C NMR** (75 MHz, CD_2Cl_2): δ = 151.8 (d, J_{C-P} = 3.5 Hz, C_q), 151.5 (d, J_{C-P} = 7.3 Hz, C_q), 150.7 (d, J_{C-P} = 1.6 Hz, C_q), 150.5 (d, J_{C-P} = 2.5 Hz, C_q), 134.1 (d, J_{C-P} = 13.0 Hz, 4 CH), 132.7 (d, J_{C-P} = 2.6 Hz, 2 CH), 130.9 (d, J_{C-P} = 5.4 Hz, CH), 129.8 (d, J_{C-P} = 11.5 Hz, CH), 129.7 (d, J_{C-P} = 2.9 Hz, 4 CH), 129.2 (d, J_{C-P} = 58.0 Hz, 2 C_q), 128.9 (d, J_{C-P} = 1.1 Hz, CH), 128.6 (d, J_{C-P} = 0.9 Hz, CH), 122.7 (d, J_{C-P} = 4.2 Hz, C_q), 118.4 (d, J_{C-P} = 1.1 Hz, CH), 118.0 (d, J_{C-P} = 0.8 Hz, CH), 116.8 (d, J_{C-P} = 2.9 Hz, CH), 33.1 (d, J_{C-P} = 33.8 Hz, CH_2). **^{31}P NMR** (121 MHz. CD_2Cl_2): δ = 31.25. **IR (ATR):** $\tilde{\nu}$/cm^{-1} = 3070 (vw), 3051 (vw), 2931 (vw), 2896 (vw), 2186 (vw), 2171 (vw), 2012 (vw), 1970 (vw), 1663 (vw), 1601 (vw), 1584 (vw), 1479 (vw), 1459 (vw), 1434 (w), 1414 (w), 1379 (vw), 1327 (vw), 1304 (vw), 1266 (vw), 1198 (vw), 1148 (vw), 1098 (vw), 1067 (vw), 1044 (vw), 1026 (vw), 999 (vw), 969 (w), 908 (vw), 889 (vw), 865 (vw), 836 (vw), 802 (vw), 766 (m), 735 (vs), 721 (m), 708 (w), 691 (vs), 612 (vw), 597 (vw), 580 (vw), 554 (vw), 506 (m), 497 (w), 472 (w), 429 (w), 396 (vw), 382 (vw). **MS (EI. 70 eV)**, *m/z* (%): 582.0 (16%) $[M]^+$, 349.1 (94%) $[M - AuCl]^+$, 165.1 (100%) $[M - AuCl - PPh_2]^+$. **Elemental analysis** calculated (%) for $C_{25}H_{19}P_1AuCl$: C 51.52, H 3.29 found: C 51.77, H 3.134.

(1-(Biphenylen-1-yl)-3-ethyl-imidazol-2-yliden)gold(I) chloride (20). A Schlenk tube was charged with **17b** (130 mg, 0.46 mmol, 1.10 eq.) and Ag_2O (165 mg, 0.71 mmol, 1.70 eq.). CH_2Cl_2 (40 ml) was added and the resulting mixture was stirred for 16 h in the dark at room temperature. After filtration through a plug of Celite® [(THT)AuCl] (135 mg, 0.42 mmol, 1.00 eq.) was added upon which a white solid immediately precipitated. The mixture was stirred for 3 h in the dark and then filtered. The filtrate was evaporated to dryness, taken up in CH_2Cl_2 (4 ml), again filtered and layered with *n*-hexane. After two weeks, colourless crystals formed. The supernatant solution was removed and the crystals were dried *in vacuo* (175 mg, 88%). **M.p.** = 163 °C (Z). **^{1}H NMR** (300 MHz, CD_2Cl_2): δ = 7.26 (dd, J = 8.7, 0.6 Hz, 1 H), 7.22 (d, J = 2.0 Hz, 1 H), 7.19 (d, J = 2.0 Hz, 1 H), 6.94 (dd, J = 8.7, 6.8 Hz, 1 H), 6.86 (ddd, J = 8.2, 6.6, 1.2 Hz, 1 H), 6.86–6.74 (m, 1 H), 6.75 (dt, J = 6.6, 1.1 Hz, 1 H), 6.73 (dd, J = 6.8, 0.5 Hz, 1 H), 6.68 (dt, J = 6.6, 1.1 Hz, 1 H), 4.34 (q, J = 7.3 Hz, 2 H, CH_2CH_3), 1.54 (t, J = 7.3 Hz, 3 H, CH_2CH_3). **^{13}C NMR** (75 MHz, CD_2Cl_2): δ = 170.3 (C_q, $C_{(Carben)}$), 152.5 (C_q), 150.7 (C_q), 148.8 (C_q), 144.2 (C_q), 130.9 (CH), 130.0 (CH), 129.4 (C_q), 129.3 (CH), 124.8 (CH), 121.3 (2 CH), 119.2 (CH), 118.9 (CH), 118.0 (CH), 47.8 (CH_2), 16.8 (CH_3). **IR (ATR):** $\tilde{\nu}$/cm^{-1} = 3169 (vw). 3129 (vw). 3096 (vw). 2983 (vw). 2185 (vw). 1704 (vw). 1668 (vw). 1588 (vw). 1470 (w). 1450 (w). 1425 (w). 1407 (w). 1380 (vw). 1357 (vw). 1315 (vw). 1268 (w). 1258 (w). 1213 (w). 1156 (w). 1138 (vw). 1110 (vw). 1090 (vw). 1051 (vw). 979 (vw). 951 (vw). 921 (vw). 895 (vw). 874 (vw). 850 (vw). 799 (w). 765 (vw). 739 (vs). 703 (m). 688 (w). 674 (w). 644 (vw). 609 (w). 541 (vw). 486 (vw). 423 (vw). 385 (vw). **MS (ESI)**, *m/z* (%): 448.3 (28%) $[M - C_2H_6]^+$. **Elemental analysis** calculated (%) for $C_{17}H_{14}N_2AuCl$: C 42.65, H 2.95, N 5.85 found: C 41.86, H 2.848, N 5.79.

[(IPr)Au(I)(2-(biphenylen-1-yl)pyridyl)][SbF$_6$] (21). In a Schlenk tube [IPrAuCl] (50 mg, 0.08 mmol, 1.00 eq.), **21** (20 mg, 0.09 mmol, 1.10 eq.) and $Ag[SbF_6]$ (31 mg, 0.09 mmol, 1.10 eq.) were dissolved in CH_2Cl_2 (2 ml). After stirring for 10 min the mixture was filtered and the filtrate was layered with *n*-hexane. After one week yellow needles formed. The supernatant solution was removed and the needles were dried *in vacuo* (33 mg, 40%). **M.p.** = 178 °C (Z). **^{1}H NMR** (300 MHz, CD_2Cl_2): δ = 8.04 (td, J = 7.8, 1.7 Hz, 1 H), 7.69 (ddd, J = 5.7, 1.6, 0.8 Hz, 1 H), 7.66–7.56 (m, 3 H), 7.47 (ddd, J = 7.6, 5.7, 1.5 Hz, 1 H), 7.40–7.28 (m, 6 H), 6.83 (ddd, J = 8.0, 7.0, 0.9 Hz, 1 H), 6.75–6.69 (m, 2 H), 6.69–6.64 (m, 1 H), 6.58–6.51 (m, 1 H), 6.37 (dt, J = 6.9, 0.9 Hz, 1 H), 6.21 (dd, J = 8.5, 6.9 Hz, 1 H), 2.50 (hept, J = 6.9 Hz, 4 H), 1.23 (d, J = 4.9 Hz, 12 H), 1.21 (dd, J = 4.9 Hz, 12 H). **^{13}C NMR** (75 MHz, CD_2Cl_2): δ = 168.4 (C_q, $C_{(Carben)}$), 158.0 (C_q), 151.9 (C_q), 151.4 (CH), 151.3 (C_q), 150.4 (C_q), 149.5 (C_q), 146.2 (4 C_q), 141.9 (CH), 134.1 (2 C_q), 131.8 (2 CH), 130.3 (CH), 130.1 (CH), 129.5 (CH), 129.4 (CH), 127.5 (C_q), 127.1 (CH), 126.2 (CH), 125.6 (CH), 125.2 (CH), 125.1 (4 CH), 119.1 (CH), 118.9 (CH), 118.5 (CH), 29.4 (4 $CH(CH_3)_2$), 24.8 (4 CH_3), 24.3 (4 CH_3). **IR (ATR):** $\tilde{\nu}$/cm^{-1} = 2960 (vw). 2927 (vw). 2870 (vw). 1607 (vw). 1566 (vw). 1551 (vw). 1470 (w). 1423 (vw). 1387 (vw). 1366 (vw). 1330 (vw). 1287 (vw). 1256 (vw). 1215 (vw). 1182 (vw). 1154 (vw). 1120 (vw). 1060 (vw). 967 (vw). 949 (vw). 936 (vw). 807 (w). 783 (vw). 764 (m). 738 (m). 706 (w). 654 (vs). 550 (vw). 507 (vw). 451 (vw). 417 (vw). 394 (vw). **MS (ESI)**, *m/z* (%): 814.3 (20%) $[M]^+$, 653.3 $[M - (i\text{-}Pr)_2Ph]^+$. **Elemental analysis** calculated (%) for $C_{44}H_{47}N_3AuSbF_6$: C 50.30, H 4.51, N 4.00 found: C 49.11, H 3.931, N 3.75.

[Bis(1-(biphenylen-1-yl)-3-ethyl-1,3-dihydro-2*H*-imidazol-2-yliden)gold(I)] triflate (23). In a Schlenk tube **20** (48 mg, 0.10 mmol, 1.00 eq.) was dissolved in CH_2Cl_2 (2 ml) and treated with Tl[OTf] (43 mg, 0.12 mmol, 1.20 eq.) upon which a white precipitate (TlCl) and colloidal gold formed. The mixture was stirred for 12 h in the dark and filtered. The filtrate was layered with *n*-hexane. After one week colourless

Open Access Article. Published on 09 June 2021. Downloaded on 9/19/2024 5:25:24 AM.
This article is licensed under a Creative Commons Attribution-NonCommercial 3.0 Unported Licence.

needles formed. The supernatant solution was removed and the needles were dried *in vacuo* (25 mg, 30%). **^{1}H NMR** (300 MHz, CD_2Cl_2): δ = 7.28–7.25 (m, 4 H), 6.96 (d, J = 8.6 Hz, 2 H), 6.91–6.77 (m, 5 H), 6.74 (tt, J = 4.5, 1.4 Hz, 5 H), 6.64 (dd, J = 6.8, 1.1 Hz, 2 H), 4.18 (q, J = 7.3 Hz, 4 H, CH_2CH_3), 1.44 (t, J = 7.2 Hz, 6 H, CH_2CH_3). **^{13}C NMR** (75 MHz, CD_2Cl_2): δ = 182.6 (2 C_q), 152.7 (2 C_q), 150.6 (2 C_q), 148.7 (2 C_q), 144.6 (2 C_q), 131.1 (2 CH), 130.3 (2 CH), 129.5 (2 CH), 129.2 (2 C_q), 124.7 (2 CH), 122.4 (2 CH), 122.0 (2 CH), 119.3 (2 CH), 119.2 (2 CH), 118.3 (2 CH), 47.4 (2 CH_2), 17.2 (2 CH_3). **IR (ATR):** $\tilde{\nu}$/cm^{-1} = 3123 (vw), 3095 (vw), 2979 (vw), 1668 (vw), 1607 (vw), 1588 (vw), 1568 (vw), 1470 (m), 1446 (w), 1417 (w), 1381 (w), 1357 (vw), 1315 (w), 1281 (m), 1261 (vs), 1222 (m), 1157 (m), 1140 (s), 1104 (w), 1088 (w), 1055 (w), 1031 (s), 976 (w), 964 (w), 928 (w), 898 (w), 822 (w), 800 (w), 774 (w), 744 (vs), 704 (m), 694 (m), 671 (w), 634 (vs), 604 (m), 572 (m), 548 (w), 536 (w), 517 (s), 496 (w), 474 (w), 448 (m), 436 (m), 423 (m), 411 (m), 395 (s), 386 (s). **MS (ESI)**, m/z (%): 689.2 $[M]^+$. **Elemental analysis** calculated (%) for $C_{35}H_{28}N_4AuSO_3F_3$: C 50.13, H 3.37, N 6.68 found: C 47.61, H 3.211, N 6.69.

General procedure for oxidative addition experiments. In a glovebox the Au(I) complex (0.02–0.2 mmol) or the Au(I) precursor and the ligand (equimolar), respectively, were dissolved in 0.5–5 ml of solvent (deuterated solvents were used for the direct monitoring of reactions *via* NMR). Additives (equimolar) and the chloride abstraction reagent (1.1 equivalents) were added and the resulting mixture was stirred inside a Schlenk tube or shaken inside a NMR tube. If performed in a Schlenk tube, the mixture was stirred (5 min–24 h), filtered, evaporated to dryness and analyzed by NMR spectroscopy.

X-ray diffraction analysis

To avoid degradation, single crystals were mounted in perfluoropolyalkylether-oil on top of the edge of an open Mark tube and then brought in contact with the cold nitrogen stream of a low-temperature device (Oxford Cryosystems Cryostream unit) so that the oil solidified. Diffraction data were measured using a Stoe IPDS II diffractometer (graphite-monochromated MoK_α (0.71073 Å) radiation). The structures were solved by dual-space direct methods with SHELXT,[79] followed by full-matrix least-squares refinement using SHELXL-2014/7.[80] All non-hydrogen atoms were refined anisotropically, with organic hydrogen atoms placed in calculated positions using a riding model. Absorption corrections were applied for all compounds (numerical). Crystallographic data (excluding structure factors) for the structures in this paper have been deposited with the Cambridge Crystallographic Data Centre.

CCD-numbers of structures contained in this manuscript: **11** 2018371, **19** 2018369, **S1** 2018372, **20** 2018370, **23** 2018373.

Computational details

All quantum chemical calculations except for solvent effects (*vide infra*) were performed with the TURBOMOLE[81,82] program package (version 7.4). Fine integration grids (m4) and SCF convergence criteria of 10^{-8} a.u., density convergence $\leq 10^{-7}$, and Cartesian gradient $\leq 10^{-4}$ were used. The TURBOMOLE module AOFORCE[83] (analytically frequency calculations) was used. All optimized structures were checked for minima (no imaginary frequencies) or transition states (one imaginary frequency according to the bond-forming and -breaking processes connecting the respective minima). Thermal Gibbs free energy contributions with inclusion of zero point energies (ZPE) were calculated at 298 K and 1 bar with the TURBOMOLE module FREEH based on assumptions of statistical thermodynamics of an ideal gas and added to the total gas-phase electronic energies. Except for the Toste system, Gibbs free energies of solvation were calculated by means of single point calculations at the same level of theory as mentioned above with the gas phase optimized structures employing the SMD[72] solvation model as implemented in ORCA 4.1.2.[84,85] A detailed description about this kind of solvent effect inclusion can be found in the literature.[86]

For the Toste system, all structure optimizations were done with the inclusion of solvent effects by the C-PCM solvation model using a Gaussian charge scheme with scaled van der Waals cavities as implemented in the ORCA 4.2.0 program package.[87] The RIJCOSX-approximation was used for these calculations.[88] We note that all structures were checked to be global minima or a transition state by inspection of the numerical hessian. The respective gas-phase optimized structures did not show any imaginary frequencies. However, upon inclusion of solvent effects, in few cases up to two small imaginary frequencies (<15 cm^{-1}) corresponding to movements of the whole cationic or anionic fragment were identified. These frequencies were neglected for the calculation of thermodynamic properties. Thermodynamics in solution phase were calculated assuming concentrations of 1 mol L^{-1} at 298 K.

The discrepancy between electronic and Gibbs free energy upon water coordination to **3*** (Scheme 10) may be understood by a common problem when dealing with association reactions and their thermochemistry: structure optimizations may be done on separate species.[89] An association then results in a huge increase of entropy due to the loss of translational and rotational degrees of freedom. In solution this can lead to errors in the calculated entropy of up to 60 kJ mol^{-1}.[90] In solution, reactions only take place when reactants approach each other in the same solvent cage, thus, the majority of translational and rotational degrees of freedom are already suppressed due to interactions with solvent molecules. Therefore, the calculation of reactant complexes according to a (hypothetical) situation of not or only weakly interacting reactants is advisable.[91] Unfortunately, for the association of complex **3*** and water, we did not find any reasonable reactant complex. Even though the described entropy-related problem may to some extent be covered by the solvation model,[86] −37 kJ mol^{-1} found for the association of water to complex **3*** probably contains a notable error.

Conflicts of interest

There are no conflicts to declare.

Open Access Article. Published on 09 June 2021. Downloaded on 9/19/2024 5:25:24 AM.
This article is licensed under a Creative Commons Attribution-NonCommercial 3.0 Unported Licence.

Acknowledgements

W. F. thanks the Carl-Zeiss Stiftung for a PhD scholarship as well as the Studienstiftung des Deutschen Volkes for general support.

References

1 S. Lamansky, P. Djurovich, D. Murphy, F. Abdel-Razzaq, H. E. Lee, C. Adachi, P. E. Burrows, S. R. Forrest and M. E. Thompson, *J. Am. Chem. Soc.*, 2001, **123**, 4304–4312.
2 Y. Kawamura, K. Goushi, J. Brooks, J. J. Brown, H. Sasabe and C. Adachi, *Appl. Phys. Lett.*, 2005, **86**, 071104.
3 H. J. Bolink, E. Coronado, S. Garcia Santamaria, M. Sessolo, N. Evans, C. Klein, E. Baranoff, K. Kalyanasundaram, M. Graetzel and M. K. Nazeeruddin, *Chem. Commun.*, 2007, 3276–3278, DOI: 10.1039/b707879j.
4 P. N. Lai, C. H. Brysacz, M. K. Alam, N. A. Ayoub, T. G. Gray, J. Bao and T. S. Teets, *J. Am. Chem. Soc.*, 2018, **140**, 10198–10207.
5 H. Rudmann, S. Shimada and M. F. Rubner, *J. Am. Chem. Soc.*, 2002, **124**, 4918–4921.
6 S. Welter, K. Brunner, J. W. Hofstraat and L. De Cola, *Nature*, 2003, **421**, 54–57.
7 Y. Chi and P. T. Chou, *Chem. Soc. Rev.*, 2007, **36**, 1421–1431.
8 M. A. Baldo, D. F. O'Brien, Y. You, A. Shoustikov, S. Sibley, M. E. Thompson and S. R. Forrest, *Nature*, 1998, **395**, 151–154.
9 M. Hissler, J. E. McGarrah, W. B. Connick, D. K. Geiger, S. D. Cummings and R. Eisenberg, *Coord. Chem. Rev.*, 2000, **208**, 115–137.
10 S. C. Kui, F. F. Hung, S. L. Lai, M. Y. Yuen, C. C. Kwok, K. H. Low, S. S. Chui and C. M. Che, *Chem. – Eur. J.*, 2012, **18**, 96–109.
11 E. Turner, N. Bakken and J. Li, *Inorg. Chem.*, 2013, **52**, 7344–7351.
12 C. Cebrian and M. Mauro, *Beilstein J. Org. Chem.*, 2018, **14**, 1459–1481.
13 C. Lee, R. Zaen, K. M. Park, K. H. Lee, J. Y. Lee and Y. Kang, *Organometallics*, 2018, **37**, 4639–4647.
14 K. M. Wong, X. Zhu, L. L. Hung, N. Zhu, V. W. Yam and H. S. Kwok, *Chem. Commun.*, 2005, 2906–2908, DOI: 10.1039/b503315b.
15 V. K. Au, K. M. Wong, D. P. Tsang, M. Y. Chan, N. Zhu and V. W. Yam, *J. Am. Chem. Soc.*, 2010, **132**, 14273–14278.
16 V. K. Au, D. P. Tsang, K. M. Wong, M. Y. Chan, N. Zhu and V. W. Yam, *Inorg. Chem.*, 2013, **52**, 12713–12725.
17 M. C. Tang, D. P. Tsang, M. M. Chan, K. M. Wong and V. W. Yam, *Angew. Chem., Int. Ed.*, 2013, **52**, 446–449.
18 M. C. Tang, D. P. Tsang, Y. C. Wong, M. Y. Chan, K. M. Wong and V. W. Yam, *J. Am. Chem. Soc.*, 2014, **136**, 17861–17868.
19 C. H. Lee, M. C. Tang, Y. C. Wong, M. Y. Chan and V. W. Yam, *J. Am. Chem. Soc.*, 2017, **139**, 10539–10550.
20 W. P. To, D. Zhou, G. S. M. Tong, G. Cheng, C. Yang and C. M. Che, *Angew. Chem., Int. Ed.*, 2017, **56**, 14036–14041.
21 C. H. Lee, M. C. Tang, W. L. Cheung, S. L. Lai, M. Y. Chan and V. W. Yam, *Chem. Sci.*, 2018, **9**, 6228–6232.
22 L.-K. Li, M.-C. Tang, S.-L. Lai, M. Ng, W.-K. Kwok, M.-Y. Chan and V. W.-W. Yam, *Nat. Photonics*, 2019, **13**, 185–191.
23 M. C. Tang, M. Y. Leung, S. L. Lai, M. Ng, M. Y. Chan and V. Wing-Wah Yam, *J. Am. Chem. Soc.*, 2018, **140**, 13115–13124.
24 C. J. Ballhausen, N. Bjerrum, R. Dingle, K. Eriks and C. R. Hare, *Inorg. Chem.*, 1965, **4**, 514–518.
25 L. J. Andrews, *J. Phys. Chem.*, 1979, **83**, 3203–3209.
26 C. Bronner and O. S. Wenger, *Dalton Trans.*, 2011, **40**, 12409–12420.
27 E. S. Lam, W. H. Lam and V. W. Yam, *Inorg. Chem.*, 2015, **54**, 3624–3630.
28 T. von Arx, A. Szentkuti, T. N. Zehnder, O. Blacque and K. Venkatesan, *J. Mater. Chem. C*, 2017, **5**, 3765–3769.
29 R. Usón, J. Vicente, J. A. Cirac and M. T. Chicote, *J. Organomet. Chem.*, 1980, **198**, 105–112.
30 K. T. Chan, G. S. M. Tong, Q. Wan, G. Cheng, C. Yang and C. M. Che, *Chem. – Asian J.*, 2017, **12**, 2104–2120.
31 L. Nilakantan, D. R. McMillin and P. R. Sharp, *Organometallics*, 2016, **35**, 2339–2347.
32 B. David, U. Monkowius, J. Rust, C. W. Lehmann, L. Hyzak and F. Mohr, *Dalton Trans.*, 2014, **43**, 11059–11066.
33 R. Kumar, A. Linden and C. Nevado, *Angew. Chem., Int. Ed.*, 2015, **54**, 14287–14290.
34 E. Peris and R. H. Crabtree, *Chem. Soc. Rev.*, 2018, **47**, 1959–1968.
35 H. Beucher, S. Kumar, E. Merino, W.-H. Hu, G. Stemmler, S. Cuesta-Galisteo, J. A. González, J. Jagielski, C.-J. Shih and C. Nevado, *Chem. Mater.*, 2020, **32**, 1605–1611.
36 R. Kumar, J. P. Krieger, E. Gomez-Bengoa, T. Fox, A. Linden and C. Nevado, *Angew. Chem., Int. Ed.*, 2017, **56**, 12862–12865.
37 L. Rocchigiani, J. Fernandez-Cestau, I. Chambrier, P. Hrobarik and M. Bochmann, *J. Am. Chem. Soc.*, 2018, **140**, 8287–8302.
38 W. Feuerstein, C. Holzer, X. Gui, L. Neumeier, W. Klopper and F. Breher, *Chem. – Eur. J.*, 2020, **26**, 17156–17164.
39 W. Feuerstein and F. Breher, *Chem. Commun.*, 2020, **56**, 12589–12592.
40 C. Y. Wu, T. Horibe, C. B. Jacobsen and F. D. Toste, *Nature*, 2015, **517**, 449–454.
41 J. J. Eisch, A. M. Piotrowski, K. I. Han, C. Kruger and Y. H. Tsay, *Organometallics*, 1985, **4**, 224–231.
42 B. L. Edelbach, R. J. Lachicotte and W. D. Jones, *J. Am. Chem. Soc.*, 1998, **120**, 2843–2853.
43 B. L. Edelbach, D. A. Vicic, R. J. Lachicotte and W. D. Jones, *Organometallics*, 1998, **17**, 4784–4794.
44 T. Schaub and U. Radius, *Chem. – Eur. J.*, 2005, **11**, 5024–5030.
45 T. Schaub, M. Backes and U. Radius, *Organometallics*, 2006, **25**, 4196–4206.
46 M. Joost, L. Estevez, K. Miqueu, A. Amgoune and D. Bourissou, *Angew. Chem., Int. Ed.*, 2015, **54**, 5236–5240.

 This journal is © The Royal Society of Chemistry 2021

Open Access Article. Published on 09 June 2021. Downloaded on 9/19/2024 5:25:24 AM.
This article is licensed under a Creative Commons Attribution-NonCommercial 3.0 Unported Licence.

47 J. Chu, D. Munz, R. Jazzar, M. Melaimi and G. Bertrand, *J. Am. Chem. Soc.*, 2016, **138**, 7884–7887.
48 A. Zeineddine, L. Estevez, S. Mallet-Ladeira, K. Miqueu, A. Amgoune and D. Bourissou, *Nat. Commun.*, 2017, **8**, 565.
49 Y. Koga, M. Kamo, Y. Yamada, T. Matsumoto and K. Matsubara, *Eur. J. Inorg. Chem.*, 2011, 2869–2878, DOI: 10.1002/ejic.201100055.
50 S. M. Kilyanek, X. D. Fang and R. F. Jordan, *Organometallics*, 2009, **28**, 300–305.
51 F. Leroux, L. Bonnafoux and F. Colobert, *Synlett*, 2010, 2953–2955.
52 L. Bonnafoux, F. R. Leroux and F. Colobert, *Beilstein J. Org. Chem.*, 2011, **7**, 1278–1287.
53 S. M. H. Kabir and M. Iyoda, *Synthesis*, 2000, 1839–1842, DOI: 10.1055/s-2000-8239.
54 R. A. Altman and S. L. Buchwald, *Org. Lett.*, 2006, **8**, 2779–2782.
55 S. Grundemann, A. Kovacevic, M. Albrecht, J. W. Faller and R. H. Crabtree, *J. Am. Chem. Soc.*, 2002, **124**, 10473–10481.
56 M. Livendahl, C. Goehry, F. Maseras and A. M. Echavarren, *Chem. Commun.*, 2014, **50**, 1533–1536.
57 R. Usón, A. Laguna, M. Laguna, B. R. Manzano, P. G. Jones and G. M. Sheldrick, *J. Chem. Soc., Dalton Trans.*, 1984, 285–292, DOI: 10.1039/dt9840000285.
58 I. Krossing, *Chem. – Eur. J.*, 2001, **7**, 490–502.
59 T. A. Engesser, C. Friedmann, A. Martens, D. Kratzert, P. J. Malinowski and I. Krossing, *Chem. – Eur. J.*, 2016, **22**, 15085–15094.
60 M. Sierka, A. Hogekamp and R. Ahlrichs, *J. Chem. Phys.*, 2003, **118**, 9136–9148.
61 V. N. Staroverov, G. E. Scuseria, J. M. Tao and J. P. Perdew, *J. Chem. Phys.*, 2003, **119**, 12129–12137.
62 J. Tao, J. P. Perdew, V. N. Staroverov and G. E. Scuseria, *Phys. Rev. Lett.*, 2003, **91**, 146401.
63 F. Weigend and R. Ahlrichs, *Phys. Chem. Chem. Phys.*, 2005, **7**, 3297–3305.
64 A. Schäfer, H. Horn and R. Ahlrichs, *J. Chem. Phys.*, 1992, **97**, 2571–2577.
65 K. Eichkorn, F. Weigend, O. Treutler and R. Ahlrichs, *Theor. Chem. Acc.*, 1997, **97**, 119–124.
66 Y. Minenkov, A. Singstad, G. Occhipinti and V. R. Jensen, *Dalton Trans.*, 2012, **41**, 5526–5541.
67 P. Rydberg and L. Olsen, *J. Phys. Chem. A*, 2009, **113**, 11949–11953.
68 S. Grimme, J. Antony, S. Ehrlich and H. Krieg, *J. Chem. Phys.*, 2010, **132**, 154104.
69 S. Grimme, S. Ehrlich and L. Goerigk, *J. Comput. Chem.*, 2011, **32**, 1456–1465.
70 S. Dohm, A. Hansen, M. Steinmetz, S. Grimme and M. P. Checinski, *J. Chem. Theory Comput.*, 2018, **14**, 2596–2608.
71 F. Jensen, *Introduction to computational chemistry*, John wiley & sons, 2017.
72 A. V. Marenich, C. J. Cramer and D. G. Truhlar, *J. Phys. Chem. B*, 2009, **113**, 6378–6396.
73 A. S. Hashmi and G. J. Hutchings, *Angew. Chem., Int. Ed.*, 2006, **45**, 7896–7936.
74 G. Dong, *Topics in Current Chemistry*, Springer Berlin, 2014.
75 A. B. Chaplin, R. Tonner and A. S. Weller, *Organometallics*, 2010, **29**, 2710–2714.
76 V. Barone and M. Cossi, *J. Phys. Chem. A*, 1998, **102**, 1995–2001.
77 Y. Yang, L. Eberle, F. F. Mulks, J. F. Wunsch, M. Zimmer, F. Rominger, M. Rudolph and A. S. K. Hashmi, *J. Am. Chem. Soc.*, 2019, **141**, 17414–17420.
78 D. F. Shriver and M. A. Drezdzon, *The manipulation of air-sensitive compounds*, Wiley, New York, 1986.
79 G. M. Sheldrick, *Acta Crystallogr., Sect. A: Found. Adv.*, 2015, **71**, 3–8.
80 G. M. Sheldrick, *Acta Crystallogr., Sect. C: Struct. Chem.*, 2015, **71**, 3–8.
81 R. Ahlrichs, M. Bar, M. Haser, H. Horn and C. Kolmel, *Chem. Phys. Lett.*, 1989, **162**, 165–169.
82 TURBOMOLE V7.4 2019, a development of University of Karlsruhe and Forschungszentrum Karlsruhe GmbH, 1989–2007, TURBOMOLE GmbH, since 2007; available from http://www.turbomole.com, 2019.
83 P. Deglmann, F. Furche and R. Ahlrichs, *Chem. Phys. Lett.*, 2002, **362**, 511–518.
84 F. Neese, *WIREs Comput. Mol. Sci.*, 2012, **2**, 73–78.
85 F. Neese, *WIREs Comput. Mol. Sci.*, 2018, **8**, e1327.
86 J. Ho and M. Z. Ertem, *J. Phys. Chem. B*, 2016, **120**, 1319–1329.
87 A. W. Lange and J. M. Herbert, *J. Chem. Phys.*, 2010, **133**, 244111.
88 F. Neese, F. Wennmohs, A. Hansen and U. Becker, *Chem. Phys.*, 2009, **356**, 98–109.
89 J. Song, E. L. Klein, F. Neese and S. Ye, *Inorg. Chem.*, 2014, **53**, 7500–7507.
90 H. Fang, H. Jing, H. Ge, P. J. Brothers, X. Fu and S. Ye, *J. Am. Chem. Soc.*, 2015, **137**, 7122–7127.
91 B. Mondal, F. Neese and S. Ye, *Inorg. Chem.*, 2015, **54**, 7192–7198.